Native Point Defects in GaN: A Hybrid-Functional Study

I. C. Diallo and D. O. Demchenko

Phys. Rev. Applied **6**, 064002 — Published 7 December 2016

DOI: 10.1103/PhysRevApplied.6.064002

Native point defects in GaN: a hybrid functional study

I. C. Diallo and D. O. Demchenko

Department of Physics, Virginia Commonwealth University, Richmond, VA 23284, USA

Abstract:

We present a systematic study of properties of common native point defects in GaN, based on hybrid density functional calculations. These defects include vacancies, interstitials, antisites, and common complexes. Using configuration coordinate diagrams, we estimate the likelihood of defects to be radiative or non-radiative. Our results show that gallium vacancies exhibit a large magnetic moment in the neutral charge state and are most likely non-radiative. This is in contrast to nitrogen vacancies, which are probable sources of the experimentally observed green luminescence band (GL2) peaking at 2.35 eV in undoped GaN. We also show that infrared photoluminescence (PL) bands that are created by 2.5 MeV electron irradiation in GaN can be explained by the formation of native defects. Namely, the interstitial gallium is likely to be responsible for the narrow infrared PL band centered around 0.85 eV, with a phonon fine structure at 0.88 eV; the gallium-nitrogen divacancies are possible sources of the broad PL band with a peak at 0.95 eV.

I. INTRODUCTION

Despite the successful fabrication of efficient blue LEDs,[1] lasers,[2] and solar cells[3] based on GaN, the properties of defects in this semiconductor are not yet fully understood. Knowledge of the electronic properties of defects is important to assess their formation during material fabrication

and processing. Of particular interest, are the native point defects of GaN, such as vacancies and interstitial defects, which may form naturally during sample growth, or can be formed as a result of electron irradiation.

Some native defects, such as vacancies, have been extensively studied experimentally throughout the past two decades, while others have been less scrutinized. Isolated Ga vacancies[4] (V_{Ga}) and the possible complexes with oxygen donors (V_{Ga}-O_N)[5,6] have been experimentally investigated by positron annihilation spectroscopy (PAS) in bulk GaN crystals and epitaxial GaN samples. Based on these experiments, Saarinen et al.[4] concluded that Ga vacancies are negatively charged in both bulk GaN crystals and layers, playing a major role in electrical compensation of *n*-type GaN. Later, Oila et al.[7] using PAS demonstrated that negatively charged Ga vacancy is the most stable acceptor defect in *n*-type GaN grown by hydride vapor phase epitaxy (HVPE). Optical properties of Ga vacancies and related complexes were also investigated, and an apparent correlation of the yellow luminescence (YL) intensity with the concentration of Ga vacancies was suggested.[4,8,9] However, other experimental studies have shown that vacancies of Ga alone do not account for the YL observed in GaN, with the possibility that carbon-related defects are involved as well.[10,11]

Among other native defects, interstitial Ga has also been extensively studied experimentally. In 2.5 MeV electron-irradiated GaN epilayers, optically detected magnetic resonance (ODMR) signals at 1.5 K were observed in PL bands peaking at ~0.85 eV and ~0.95 eV. [12] Based on the obtained resolved hyperfine structure, it was suggested that the microscopic origin of one of the ODMR signals was a complex formed by interstitial Ga and another unidentified defect. Further ODMR studies on the 0.85 eV PL band were performed by Buyanova et al.[13] at 2 K and 30 K. It was shown that the defect responsible for the 0.85 eV PL

band has its principal symmetry axis along the *c*-axis of wurtzite GaN. Bozdog et al.[14] performed ODMR studies at room temperature on electron–irradiated GaN samples, also observing the two infrared (IR) bands centered at 0.85 eV and 0.95 eV. Two out of the three observed EPR signals revealed strong hyperfine interaction with a single Ga nucleus, suggesting that they are related to the isolated interstitial Ga. More recent ODMR studies on electron-irradiated GaN samples were performed at various temperatures by Watkins et al. [15] and Chow et al.,[16,17] where only the broad 0.95 eV PL band was observed from 4.2 K (*in-situ* irradiation) up to 295 K. Two of the obtained ODMR signals were attributed to the isolated interstitial Ga located in either octahedral or tetrahedral sites in GaN. Above 295 K, the 0.95 eV PL band lost 80-90% of its intensity while the sharp 0.85 eV PL band and its characteristic ODMR signal started emerging. The changes of ODMR signals band were explained by the possible migration of interstitial Ga near the vacant Ga site, from which they were created by electron irradiation. However, despite thorough experimental studies of the effect of electron irradiation on the properties of GaN, the microscopic origin of the near IR PL bands peaking at 0.85 eV and 0.95 eV is still not entirely clear.

Electrical and optical properties of nitrogen vacancies (V_N) and related complexes were also investigated in recent experiments, mostly in Mg-doped *p*-type GaN.[18,19,20] Nitrogen vacancies associated with magnesium acceptors (V_N-Mg_{Ga}), were identified by Hautagankas et al.[18] using positron annihilation spectroscopy (PAS) in Mg-doped GaN. It was suggested that V_N-Mg_{Ga} complexes behave as compensating centers in *p*-type GaN, and that vacancies of Ga and N are abundant in both *n*-type and *p*-type GaN. Using a combination of ODMR and PAS experiments, Zeng et al.[19] suggested that the red PL band peaking at 1.80 eV in Mg-doped GaN is caused by the donor-acceptor pair recombination, where electrons localized on deep donor V_N-

Mg_{Ga} complexes recombine with holes on deep V_{Ga} acceptors. Further investigation of the optical properties of nitrogen vacancies performed by Reshchikov et al.[20] using PL spectroscopy, proposed that V_N is the best candidate for the green luminescence band (labeled GL2) occurring at 2.35 eV in high-resistivity undoped and Mg-doped GaN. However, it was noted that N vacancy is present with relatively low concentrations in both types of samples.

While positron annihilation allows detection of vacancies, the experimental identification and characterization of other types of native defects (interstitials, antisites) have been proven difficult. Other experimental techniques, such as ODMR or PL spectroscopy provide only certain partial information about the nature and properties of these native defects. Therefore, sparse (and in some cases contradictory) experimental data suggests that revisiting the basic questions of native defects in GaN from the theoretical point of view is in order.

Theoretical investigations of native defects in GaN have been performed using various methods, such as tight binding approximation[21], empirical potential methods[22], ab-initio Molecular Dynamics[23], and the density functional theory (DFT).[24,25,26,27] Early atomistic theoretical studies of the electronic structure of vacancies and antisites in GaN were performed by Jenkins and Dow[21] using the tight binding approximation. It was shown that N vacancy is a shallow donor in GaN, also creating a doubly occupied deep level within the band gap. Further analysis on intrinsic defects using DFT was performed in Refs. [24-26,28] where it was found that the most stable native defects in GaN are the compensating defects, i.e. donor nitrogen vacancies in *p*-type GaN and acceptor Ga vacancies in *n*-type GaN. Antisites and interstitial native defects were found to be less favorable. Other theoretical calculations based on the local density approximation (LDA)[29] using scissor corrections agreed well with previous predictions of the deep acceptor properties of V_{Ga} but unexpectedly predicted the existence of both donor

and acceptor states (up to 3- charge state) for nitrogen vacancy.[27] Similar DFT calculations performed in Ref. [30] suggested that V_N should be the dominant defect in both *p*-type and *n*-type GaN annealed samples.

Although less studied than vacancies, antisites and native interstitials were also addressed by theory, producing varying results. By using both DFT and empirical potential methods, Gao et al.[22] obtained the formation energy of neutral antisite N_{Ga} which agreed with the value obtained by Gorczyca et al.[31] where the Green's function technique[32] was used. However, these results were significantly higher than the DFT values obtained by Neugebauer et al.[24] In the case of neutral Ga interstitial, the results obtained using empirical potential methods (Ref. [22]) also differ from previous ab-initio calculations performed in Refs. [24-26, 28**].**

In addition to isolated intrinsic defects, properties of di- and trivacancies in bulk GaN were also investigated. DFT calculations performed in Ref. [27] showed that Ga-N mixed divacancy ($V_{Ga}V_N$) behaved as a deep acceptor center. The calculations yielded the divacancy formation energy lower than that of V_{Ga}, with a substantial binding energy of 2.34 eV (for Fermi energy $E_F > 1.5\,\text{eV}$). However, more recent generalized gradient approximation (GGA)[33] calculations performed by Gohda et al.[34] and Puzyrev et al.[35] suggested that divacancies display both donor and acceptor properties and are less energetically stable than V_{Ga} in *n*-type GaN (with the energy difference ~1 eV). Trivacancies ($V_{Ga}V_NV_{Ga}$) were also investigated in Ref. [34], where it was shown that $V_{Ga}V_NV_{Ga}$ are unstable in *p*-type GaN but exhibit formation energy identical to that of divacancies in *n*-type GaN.

Calculations of defect properties using local (or semi-local) approximations to the DFT are prone to inaccuracies due to the known underestimation of the band gap. Recent studies of

vacancies[36,37,38] in GaN used non-local screened exchange LDA (sX-LDA) and Heyd-Scuseria-Ernzerhof (HSE) hybrid functional, which can circumvent the band gap problem. These studies showed substantial differences in the electronic structure of defects compared to the results of the (semi)local approximations to the DFT. While considered a step forward, the results obtained with these new computational methods are also a subject of interpretation. For example, using HSE calculations, Yan et al.[36] suggested that nitrogen vacancy could be a possible source of the YL band observed in Mg-doped GaN. On the other hand, hybrid functional calculations based on sX-LDA performed by Gillen and Robertson,[37] associated the YL with the 0/- transition level of the gallium vacancy. Recent HSE calculations performed by Lyons et al.[38] proposed that while transitions via 2-/3- level of isolated V_{Ga} are most likely non-radiative, V_{Ga} complexes with oxygen and hydrogen can contribute to the YL band in GaN. Most recent HSE calculations performed in Refs. [39, 40] also describe the energetics of native defects in GaN. Both calculations indicated that in Ga-rich conditions, V_N is the most energetically stable native defect.

Overall, both experiment and theory have produced large amounts of widely varying results. On one hand, only limited information for some defects is accessible from experiments, while on the other hand, different theoretical approaches often yield conflicting results. Consequently, many details of the electronic properties of native defects in GaN remain unclear. In this paper, we perform a systematic study of the electronic and optical properties of common native defects, namely Ga vacancy (V_{Ga}), N vacancy (V_N), Ga-N divacancy ($V_{Ga}V_N$), interstitial Ga (Ga_i), Ga antisite (Ga_N), interstitial N (N_i), N antisite (N_{Ga}), the complex consisting of Ga interstitial and vacancy of Ga (Ga_iV_{Ga}), and the complex consisting of gallium antisite and vacancy of Ga (Ga_NV_{Ga}). We use a theoretical approach based on exchange tuned HSE hybrid

functional,[41] which in recent years has emerged as one of the most practical methods for calculations of defects in semiconductors. In particular for defect related optical transitions in GaN, this method has been tested against experimental results using a well understood Zn acceptor PL band,[42] and found to accurately reproduce measured thermodynamic and optical transition levels. We also summarize and compare our results to the most recent theoretical calculations of native defects in GaN, and identify the possible sources of discrepancies.

II. METHODS

First-principles calculations based on DFT within the LDA and GGA have been a prevalent tool for the analysis of electronic structure of defects in semiconductors for the past three decades.[26] However, different correction schemes for defect calculations that were developed to account for the underestimated bandgaps, often yielded conflicting results.[43] Recently, a new class of theoretical methods based on hybrid functionals has been developed, suggesting that they can circumvent these difficulties.[44] Hybrid functionals provide more reliable electronic structure of defects, and show favorable comparison of the results with experiment in GaN.[45,46,47] In order to study the electronic structure and optical properties of native defects in GaN, we use the range separated hybrid functional of Heyd, Scusseria, and Ernzherof (HSE06),[41] and the projector-augmented wave (PAW)[48] formalism as implemented in the VASP code.[49] Here, the Ga 3*d* valence electrons are not included in the PAW pseudopotentials. The HSE06 separates the Fock exchange into short-range and long-range components. In the short-range part, 75% of semilocal exchange of the Perdew-Burke-Ernzerhof (PBE)-GGA[50] is mixed with 25% of a non-local Fock-type exchange energy. In the long-range part, the exchange and correlation potentials

are described solely by the PBE functional. As typical for defect calculations in GaN, we adjusted the amount of exact exchange to 31% and the screening parameter is kept at typical 0.2 $Å^{-1}$. These parameters result in a band gap of 3.487 eV which is in a good agreement with the low temperature experimental value of 3.50 eV.[51] Calculated lattice parameters a = 3.210 Å, c = 5.198 Å and u = 0.377 Å for relaxed wurtzite GaN are also in good agreement with experimental values.[52] Good convergence was achieved using the cutoff energy of 400 eV, the Γ-point only, and hexagonal supercells containing 128 atoms. All structural relaxations were also performed within the same exchange tuned HSE to reduce forces to less than 0.05 eV/Å. Using larger supercells (up to 300 atoms) or denser **k**-point mesh (2×2×2), we estimate that above parameters produce errors of less than 0.05 eV in formation energies and transition levels.

The formation energy of a particular defect configuration *D* in the charge state *q* is given by:[26]

$$E_f\left[D^q\right] = E_{tot}\left[D^q\right] - E_{tot}\left[bulk\right] + qE_F - \sum_\alpha \Delta n_\alpha \mu_\alpha + \Delta V + \Delta E_{MP} \qquad (1.1)$$

where $E_{tot}\left[D^q\right]$ and $E_{tot}\left[bulk\right]$ are the total energies of the supercell with a defect and a bulk supercell, respectively. The third term qE_F is the energy cost to add a charge *q* to the defect, assuming that the exchange of electrons between the defect and the host material occurs at the Fermi level (E_F). The numbers of atoms of type α that have been removed from, or added to the supercell is Δn_α, and μ_α is the elemental chemical potential of the α atom. The chemical potentials depend on the growth conditions and are usually computed for Ga-rich and N-rich growth conditions, setting the limits on the values of the chemical potentials.[26] In Ga-rich (N-rich) conditions, Ga (N) chemical potential is computed from metal Ga (N_2 molecule). The

chemical potential of Ga in Ga-poor (N in N-poor) conditions is obtained by adding the GaN enthalpy of formation ($\Delta H(\mathrm{GaN})$) to the above value. Here, $\Delta H(\mathrm{GaN})$ was calculated using total energies of bulk GaN, orthorhombic metal Ga, and N_2 molecule, with volumes and atomic coordinates fully relaxed with HSE parameterization described above. The resulting $\Delta H(\mathrm{GaN}) =$ -1.249 eV is in reasonably good agreement with previous theoretical calculations[36,56] and the experimental value of -1.34 eV reported recently.[53] The two remaining terms ΔV and ΔE_{MP} correct for the electrostatic errors of two different origins. The potential alignment ΔV arises from introducing the compensating uniform charge background in a charged supercell.[43] This term is computed as a difference of the average electrostatic potential far from the defect in the supercell, and that in the bulk. This term is proportional to the defect formal charge q, and in our 128 atoms supercell can be as large as 0.18 eV, for instance for V_{Ga} in 3- charge state. However, computed transition levels are weakly affected by this term due to its partial cancellation, since a transition level is a formation energy difference. The last term ΔE_{MP} is the electrostatic correction according to Makov and Payne[54]. It arises from the artificial interactions between charged defects and compensating background charge due to periodic boundary conditions. Here we use the first order term (Madelung energy) and third order term (dipole corrections), since these two terms dominate interaction energy, following the procedure outlined by Lany and Zunger in Ref. [43. Both terms scale as the square of the charge state of the defect q^2, and although they have opposite signs, the combined values of this correction are significant; for example in our 128 atom supercells, it is 1.16 eV for a defect charge states of ±3. Following Oba et al.[55], Madelung corrections are also applied to neutral shallow defects. This is because a supercell cannot contain a shallow defect wavefunction, and in a neutral charge state a carrier (electron or hole) occupies a delocalized perturbed host state. This leads to artificial interactions,

similar to those for a charged defect in a compensating charge density, pushing shallow transition levels deeper into the bandgap. For this reason, in the literature, somewhat deep transition levels (several hundred meV) are sometimes reported for cases of shallow defect states.

Formation energy defined by Eq. (1.1) cannot be expected to yield realistic defect concentrations. One reason is that the defect concentrations are determined by the free energy of defects, and in the cases of the high temperature growth such as MOCVD, entropic contributions are significant.[56,57] However, transition levels calculated in this work are compared to PL measurements performed at low or room temperature. In this case, vibrational entropic contribution to the free energy of the defect and consequently to the defect transition level is negligible (< 0.05 eV).[56] Also, since materials are often grown in non-equilibrium conditions, the values of defect formation energy should be used as rough guidelines for defect formation. Furthermore, the presence of contaminants and growth byproducts could change chemical potential bounds by introducing additional phases limiting GaN growth, i.e. formation of ammonia or oxides in the presence of hydrogen or oxygen. These complications do not affect the results of this work, since defect transition levels are calculated from the formation energy differences.

III. RESULTS

A. VACANCIES

Gallium vacancy (V_{Ga})

Electron irradiation experiments have been shown to create large numbers of native defects, such as interstitials and vacancies.[15,70] Therefore, a natural question is whether V_{Ga} can explain infrared PL bands observed in electron irradiated GaN samples. Figure 1 (a, b) shows the formation energies of Ga vacancy in Ga-rich and N-rich growth conditions obtained from our HSE calculations. The slope of each line corresponds to a charge state of the defect, while the intersection points represent thermodynamic transition levels. We find that V_{Ga} exhibits both donor and acceptor properties, and four thermodynamic transition levels are predicted within the bandgap, namely the $\varepsilon(+/0) = 0.94$ eV, the $\varepsilon(0/-) = 1.73$ eV, the $\varepsilon(-/2-) = 1.87$ eV, and $\varepsilon(2-/3-) = 2.34$ eV, above the valence band maximum (VBM). In the singly positive charge state (+), the N atoms near the vacant Ga site, relax away from the vacancy by 12.3%, while with addition of electrons the outward distortions decrease. For instance, in the 3- charge state, the distances between neighboring N atoms and the vacant Ga site decrease by 9.38% (compared to the ideal bulk Ga-N bond length).

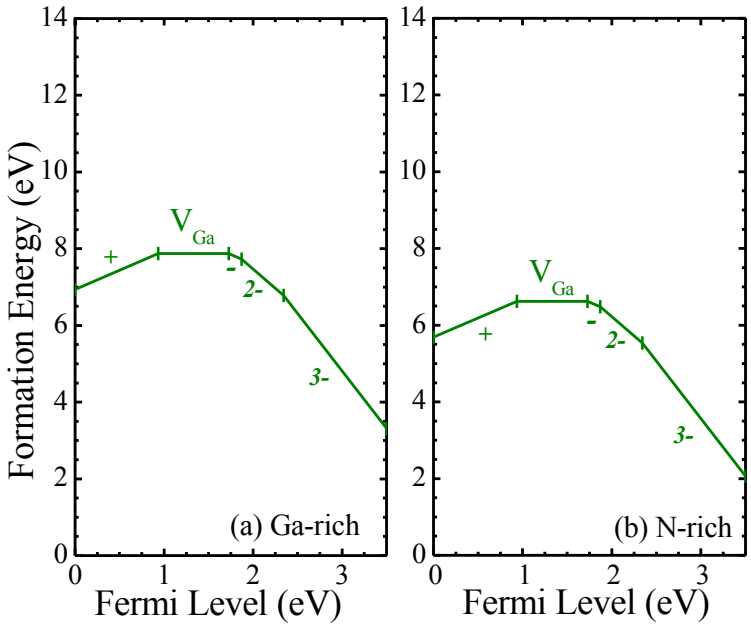

FIG. 1. Formation energy of V_{Ga} as a function of the Fermi energy in (a) Ga-rich and (b) N-rich growth conditions. The zero and maximum of the Fermi level scale correspond to the top of the valence band and the bottom of the conduction band, respectively. The solid lines correspond to the formation energies for the most stable charge states of the defects. The points where each line changes slope (charge state) mark thermodynamic transition levels in the GaN band gap.

While V_{Ga} has been widely discussed as a possible source of the yellow and green luminescence bands in GaN, the exact attribution of these PL bands is still not entirely settled. By using the configuration coordinate diagram (CCD)[58] fitted into the calculated optical transitions and lattice relaxation energies, one can estimate whether the recombination via the defect is radiative or non-radiative. An example of such CCD is schematically shown in Fig. 2. The likelihood of a non-radiative transition can be estimated by finding the point at which the two potential curves corresponding to the two charge states intersect.[59,60] The energy of this intersection with respect to the vibrational ground state of the upper curve (excited state of the

defect) represents the potential barrier for a non-radiative transition. If the resonant optical excitation occurs at a higher energy than this crossover, then the energy of the system upon excitation is higher than the barrier for a non-radiative transition. In this case there are two possible scenarios. Depending on the coherence length and time for the resulting excited vibrational state (Fig. 2), the defect can either relax into the vibrational ground state or transfer to the lower curve at the crossover point. In the latter case, the defect is likely to be non-radiative.[59] In the former case, if the barrier height $\Delta\epsilon_b$ is not too high compared to the temperature of the sample, and the radiative transition probability is low (PL lifetime is long), the system can also transition to the lower curve by thermally jumping over the barrier. Otherwise, when the barrier is too high for a thermal activation, or the lifetime of the excited state is short, (for example, due to high electron concentrations in *n*-type GaN) the recombination is likely to be radiative. The radiative and non-radiative transitions are schematically illustrated in Fig.2, using the CCD.[61] Accurate predictions of radiative versus non-radiative transition rates require calculations of electron-phonon interactions, and are currently a subject of intensive development (see for example recent Refs. [62, 63]). The method based on the intersection point between two potential curves for different charge states within the harmonic approximation has been successfully used for predicting radiative versus non-radiative transitions in F-centers in the alkali halides.[59,64,65,66] Nonetheless, this method has not been thoroughly tested in GaN, which is why here we only draw preliminary conclusions about radiative or non-radiative nature of recombination via common native defects, based on the excitation and barrier energies obtained from CCD.

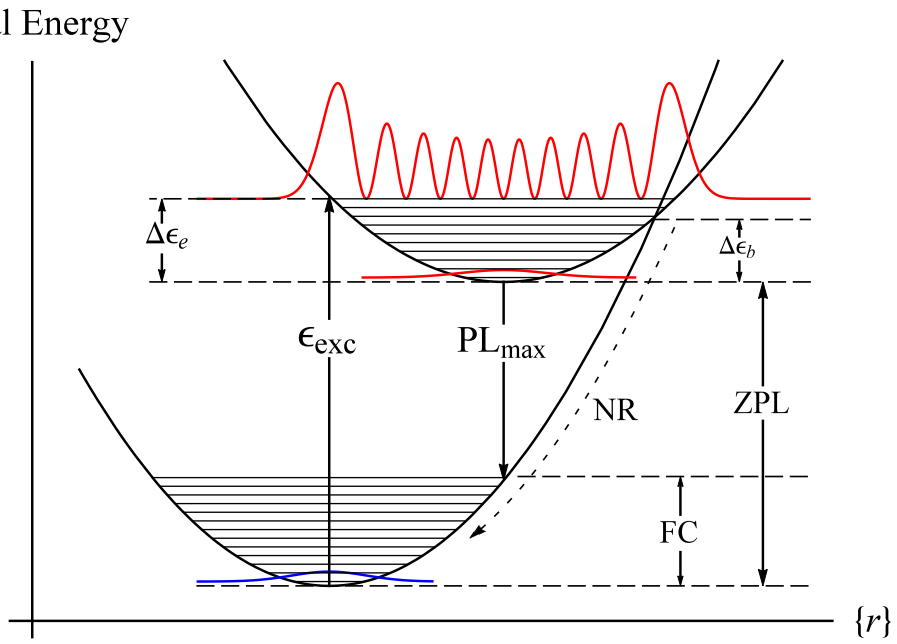

FIG. 2. Schematic configuration coordinate diagram, displaying possible radiative and non-radiative transitions between the excited and ground states of a defect. The potential curve of the excited state is vertically displaced from that of the ground state according to their formation energies and assuming the presence of an electron in the conduction band. The ZPL describes the transition between the zero-point vibrational states in excited state and ground-state configurations. ϵ_{exc} is the resonant excitation energy (absorption energy), PL_{max} corresponds to the peak of the PL band. $\Delta\epsilon_e$ and FC (Franck-Condon shift) describe the relaxation energies of the excited state and the ground state, respectively. $\Delta\epsilon_b$ (energy barrier) is the energy between the vibrational ground state of the upper curve and the crossover between the two curves. The dashed arrow labeled NR represents a non-radiative transition.

In *n*-type GaN, V_{Ga} lowest energy charge state is 3- (Fig. 1). The CCD shown in Figure 3 is based on the harmonic approximation and describes the optical transitions via the (2-/3-) level of V_{Ga}. The CCD is constructed by fitting parabolic potential curves into HSE computed total energies of the defect. The lower potential curve (V_{Ga}^{3-}) is obtained by fitting a parabola into the

two calculated total energies of the V_{Ga}^{3-} in the relaxed defect lattices of the 3- and 2- charge states (this energy difference is the calculated Franck Condon shift of 0.54 eV). The upper potential curve is also obtained in similar manner, where a parabola is fitted into the calculated total energies of the V_{Ga}^{2-} in the relaxed defect lattices of the 3- and 2- charge states (the energy difference is the calculated relaxation energy of 0.46 eV). Note that in this CCD, all optical transitions are calculated directly from HSE, while the energy crossover for the non-radiative transition relies on the harmonic approximation.

In order to demonstrate the validity of the harmonic approximation, we have also directly calculated parts of the CCD using HSE total energies of the defects between two minima points in the 3- and 2- charge states. Linear displacement was used to obtain intermediate defect geometries. As shown in Fig.3, the direct HSE calculations yielded results that are very similar to the harmonic approximation, with average energy difference of 4 meV. In case of deep defect such as V_{Ga} where distortions tend to be large, the harmonic approximation still remains an accurate approach to describing the potential curves of the CCD.

Based on the CCD shown in Fig. 3, the calculated resonant excitation $V_{Ga}^{3-} \rightarrow V_{Ga}^{2-}$ is expected to have a maximum at 1.60 eV, which is 0.33 eV higher than the intersection of the two potential curves. Losing the excess energy through phonon emission, the system can either relax into the vibrational minimum of the V_{Ga}^{2-} state, or undergo a non-radiative transition to the ground state V_{Ga}^{3-}. In the former case, the subsequent recombination of the hole localized on the vacancy and an electron from the CBM, returns the vacancy from V_{Ga}^{2-} to the V_{Ga}^{3-} state, with a PL maximum computed at 0.60 eV. This transition is then followed by lattice relaxation (FC shift) of 0.54 eV, resulting in a ZPL of 1.14 eV. However, based on the CCD (Fig. 3), the barrier

for the non-radiative transition is 0.13 eV, suggesting that at room temperature the average time of the thermal jump over this barrier is several orders of magnitude shorter than a typical defect PL lifetime. Thus, the V_{Ga} is likely non-radiative.

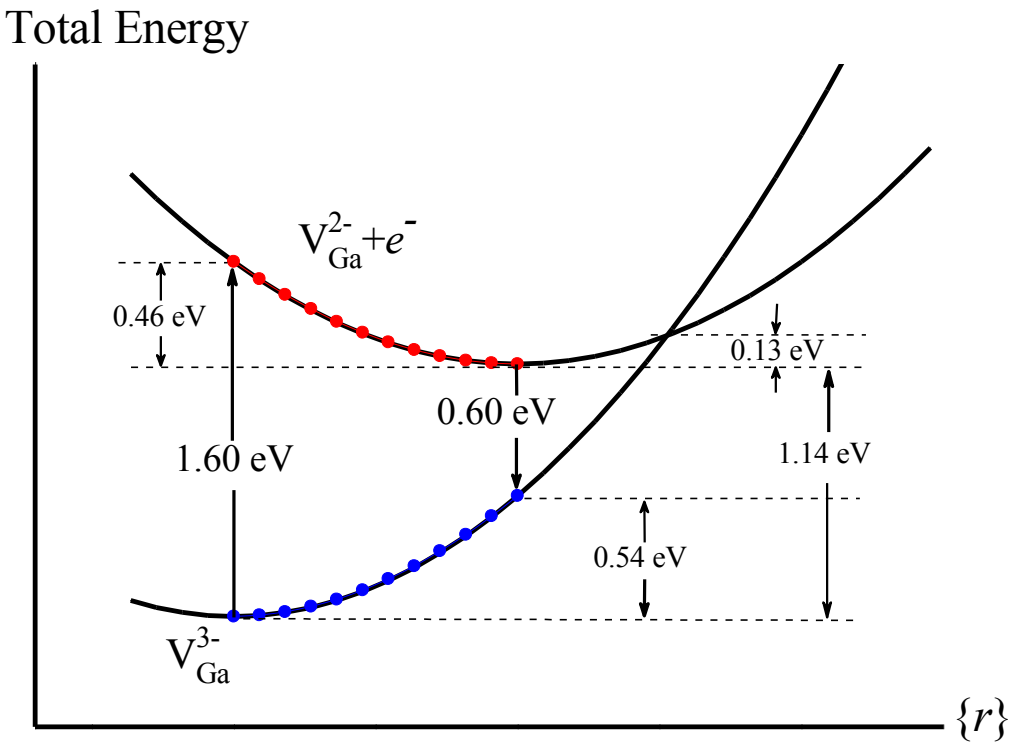

FIG. 3. Configuration coordinate diagram of V_{Ga} obtained from the harmonic approximation fitting of total energies at relaxed defect lattices only (solid black lines), and direct HSE calculations (filled circles). The filled circles correspond to the total energies of ten intermediate defect geometries between two minima in the 3- and 2- charge states. An average difference in energy of 4 meV is found between the CCD based on the harmonic approximation and the CCD obtained from direct HSE calculations. A calculated emission of 0.60 eV, a FC shift of 0.54 eV

and a ZPL of 1.14 eV are obtained. The energy barrier for a non-radiative transition is 0.13 eV, making the V_{Ga} likely non-radiative.

(a) 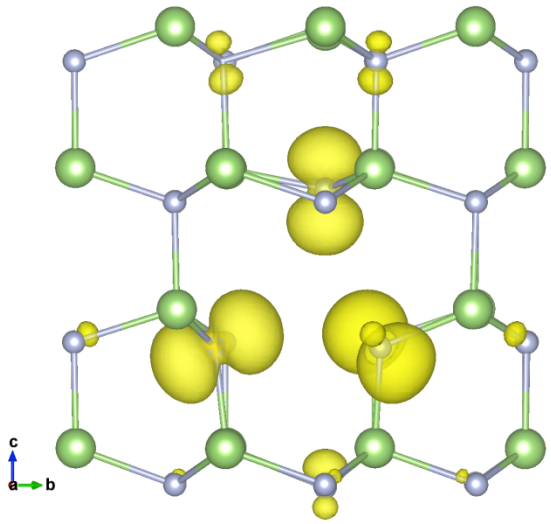	(b) 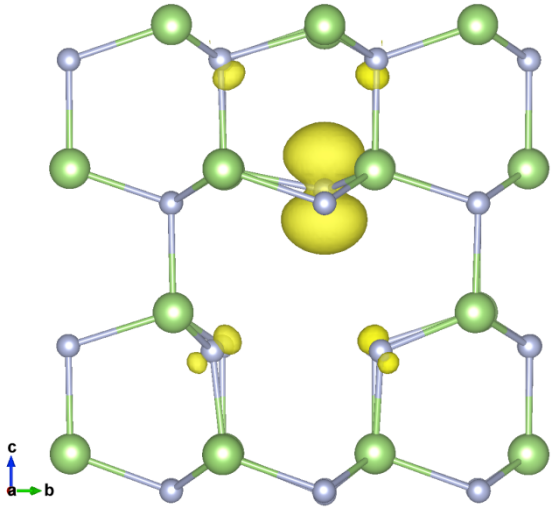
(c)	(d)

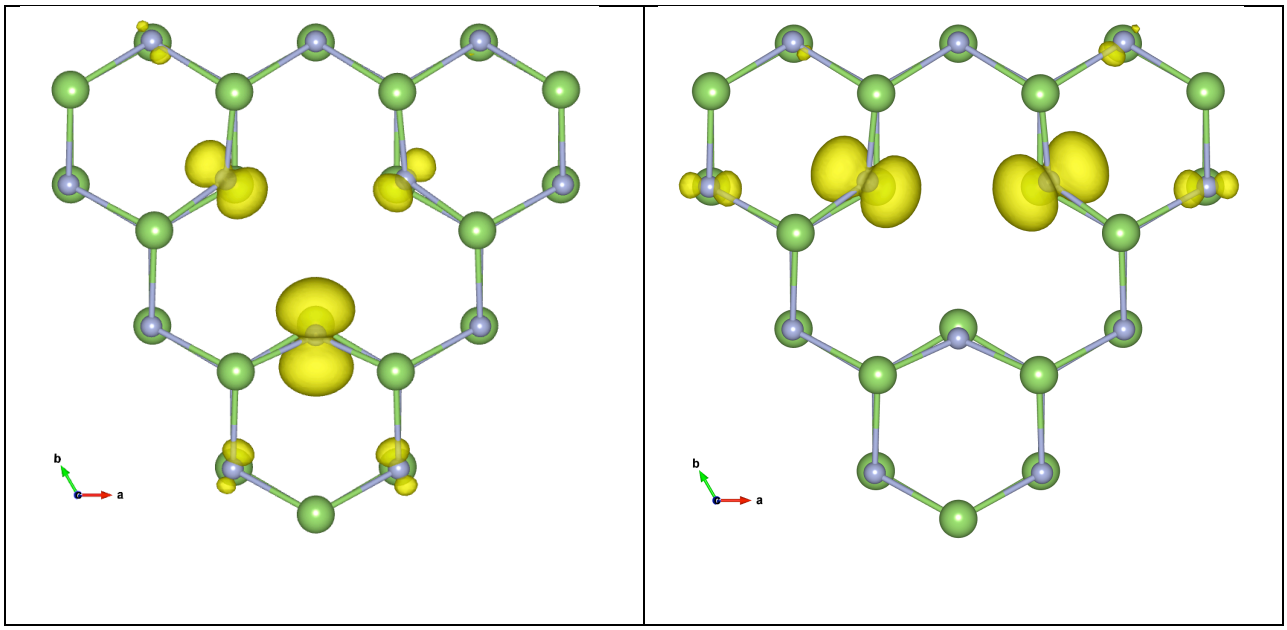

FIG. 4. Charge density isosurfaces of the four defect states of V_{Ga}. The wavefunctions are calculated in the 3- charge state of the defect. For clarity, two different orientations are used for states (a, b) and (c, d), indicated by the lattice vectors. The (a)-(d) charge densities correspond to the eigenvalues shown in Fig. 5 (right panel, 3- charge state of V_{Ga}), from lowest (a) to highest (d) energy. The small (grey) and large (green) spheres indicate the nitrogen and gallium atoms, respectively. The isosurface values are set at 5% of the maximum.

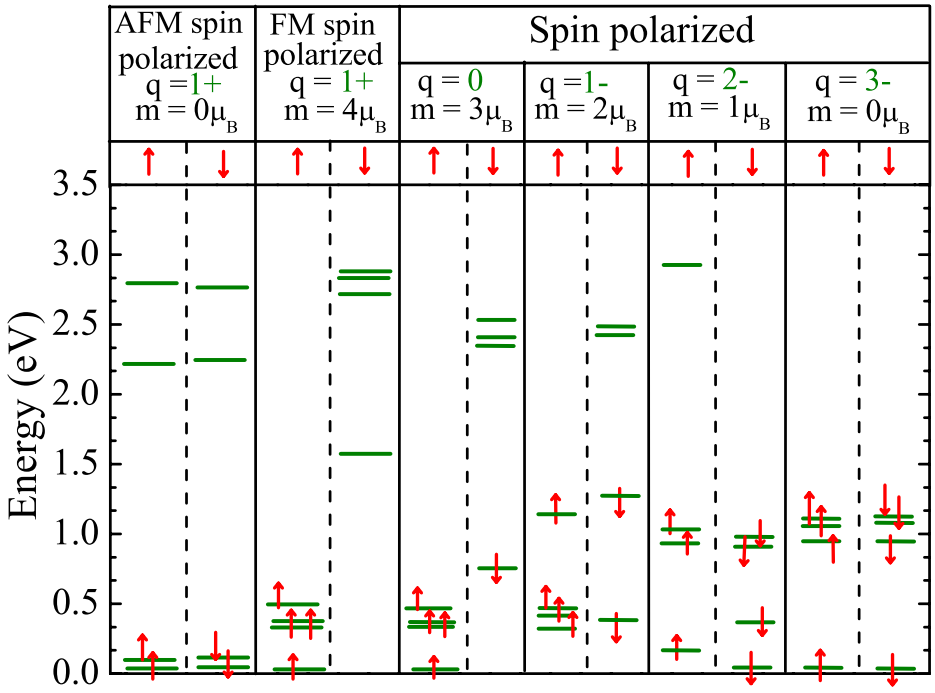

FIG. 5. Single-electron energy levels of V_{Ga} for all the possible charge states *q* with their respective magnetic moments *m*. Zero energy corresponds to the VBM.

Our calculations show that removal of Ga atom in bulk GaN, i.e. breaking four bonds with nearest N atoms, creates four defect levels within the bandgap. The atomic structure and charge density of each of the four defect levels are displayed in Fig. 4. In this example the V_{Ga} is in the 3- charge state, where all defect states are occupied by electrons. V_{Ga} defect states are linear combinations of nitrogen *p*-orbitals, which vary in the degree of localization. Each state displayed in Fig. 4 is degenerate with respect to spin. These defect states form four transition levels within the bandgap shown in Fig. 1. The HSE calculated single electron energies and their changes with addition/removal of electrons to the Ga vacancy are shown in Fig. 5. For example, in the 3- charge state, the highest energy occupied defect states (spin-up and down) are located at 1.12 eV above the VBM. When V_{Ga} traps a hole, leading to 2- charge state of the defect, the

highest spin-up state is shifted to 2.83 eV above the VBM. This, along with energy of accompanying atomic relaxations, results in the 2-/3- transition level occurring at 2.34 eV in Fig. 1. Another example is the spin-down defect state located at 1.29 eV above VBM in the 1- charge state (Fig. 5). Removing an electron from this defect state leads to the 0/- transition level at 1.68 eV in Fig 1.

As shown in Fig. 5, unpaired spins of the electrons localized at the Ga vacancy lead to the local magnetic moment of V_{Ga}. When all defect states are occupied by electrons in 3- charge state, the charge density is equally distributed over four spin-up and four spin-down states, resulting in zero magnetic moment of the vacancy. Removing one electron, i.e. introducing one hole to the highest energy spin-up state leads to the magnetic moment of 1 μ_B for the 2- charge state of the defect. In this case ~80% of magnetization is localized on one of the nearest nitrogen atoms. In the singly negative charge state, the magnetic moment is 2 μ_B, with most of the magnetization density (about 90%) localized on the three neighboring nitrogen atoms, about ~0.59 μ_B each. In this case two of the four spin-down states are occupied by electrons (Fig. 5). Finally, in 0 and + charge states of V_{Ga}, the spin-down defect states have three and four localized holes, respectively, while in both cases all spin up states are occupied by electrons. This results in the vacancy magnetic moments of 3 μ_B and 4 μ_B, in 0 and + charge states, respectively. In this case, calculations show that each of the four neighboring nitrogen atoms has local magnetic moments of 0.64 μ_B and 0.82 μ_B in 0 and + charge state respectively, and all local magnetic moments are ferromagnetically (FM) ordered. In both cases, the nearest neighbor nitrogen atoms provide ~85% of the total vacancy magnetic moment, while the remaining magnetization of the V_{Ga} comes from farther nitrogen atoms.

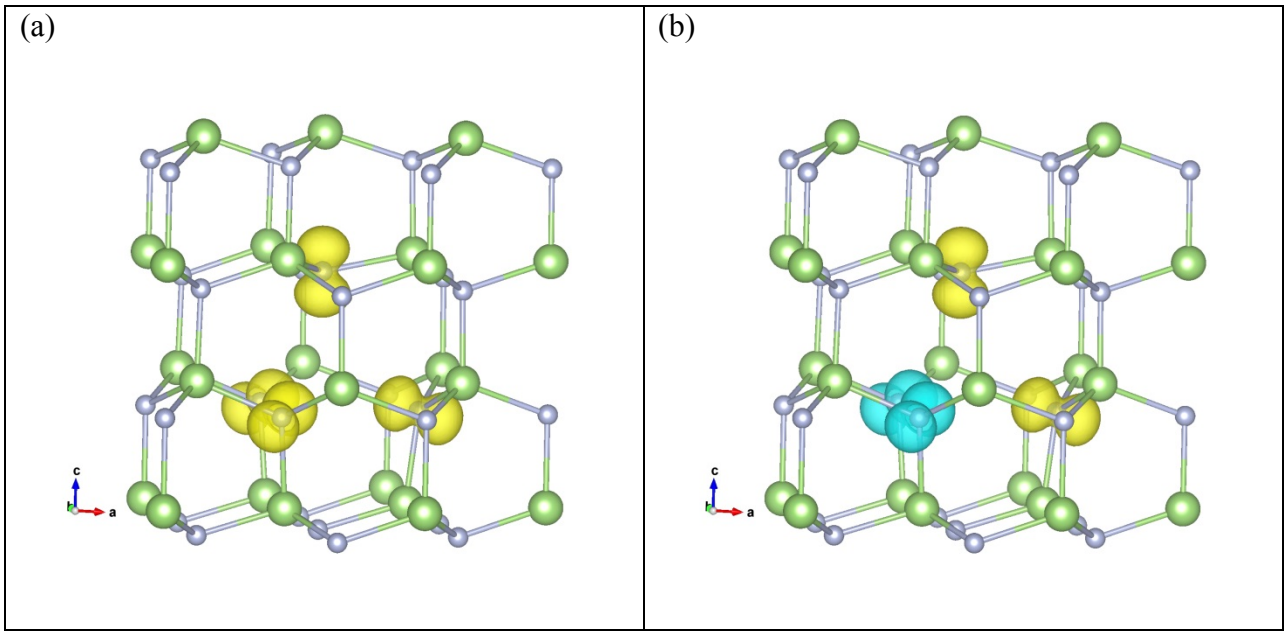

FIG. 6. Magnetization density isosurfaces of V_{Ga} in the singly positive charge state in the (a) FM spin configuration and (b) AFM spin configuration. The positive (yellow) and negative (light blue) isosurface values are plotted at 10% of the maximum. AFM spin alignment has lower energy than FM alignment by 75 meV.

Large magnetic moments of V_{Ga} in + and 0 charge state raise questions about whether these ferromagnetic alignments of spins on neighboring N atoms are of the lowest energy. HSE calculations show that the antiferromagnetic (AFM) spin configuration on the four nearest N around the vacant Ga site in the + charge state is more energetically favorable than the FM alignment by $\Delta E_f \sim 75$ meV. In AFM configuration, two of the spin-up and two of the spin-down defect states are occupied by electrons while the remaining two states of each spin have two localized holes, as shown in Fig. 5, leading to a net magnetic moment of 0 μ_B. Comparison

of the magnetization density of V_{Ga}^{+} in both AFM and FM spin configurations are displayed in Fig. 6. The defect states consisting of linear combination of *p*-orbitals localized at the four nearest N atoms create four aligned magnetic moments in the FM spin configuration (Fig. 6(a)). In the AFM configuration, each pair of the local magnetic moments is antiparallel (Fig. 6(b)). Similarly to FM case, local magnetic moments of each of the four neighboring N atoms are computed to be ~0.80 μ_B, while the remaining magnetization mostly originates from next nearest N atoms. In contrast to the + charge state, the magnetic moment of 3 μ_B in the neutral charge state of V_{Ga} is more energetically favorable with respect to the possible AFM alignment by 47.5 meV. Thus, following Fig. 1, in *p*-type or high resistivity samples, V_{Ga} is predicted to have a magnetic moment of zero for Fermi energies up to 0.94 eV above the VBM, then a large 3 μ_B for Fermi levels between 0.94 eV and 1.73 eV, 1 μ_B for Fermi levels between 1.87 eV and 2.34 eV, and zero again for Fermi levels over 2.34 eV above the VBM.

According to Fig. 1 (a,b) for Fermi level close to the CBM, Ga vacancies exhibit the lowest formation energy among all investigated native defects in all growing environments. This indicates that V_{Ga} can play a role as a compensating center in *n*-type GaN, which is consistent with previous experimental predictions.[4] In all other kinds of samples, i.e, high resistivity, *p*-type and compensated GaN, isolated vacancies of Ga exhibit fairly high formation energies and are unlikely to occur, unless created by electron irradiation.

Nitrogen vacancy (V_N)

Figure 7 shows formation energies of the nitrogen vacancy (V_N) in the lowest energy charge states + and 3+. HSE calculated 2+/+ and 3+/2+ transition levels are located at 0.47 eV and 0.61 eV above the VBM, respectively. The formation energy of the 2+ charge state is always higher than the + and 3+ charge states, hence V_N exhibits properties of a negative-*U* center (with U = -0.13 eV). The crossover 3+/+ occurs at 0.54 eV above the VBM, which is between the value of 0.47 eV reported in Refs. [36, 40] and the value of 0.70 eV obtained in recent HSE calculations.[56] Overall, nitrogen vacancy is a donor defect with both deep and shallow levels. Relatively high formation energy of V_N for Fermi-level positions near the CBM indicates that nitrogen vacancies are unlikely to be an effective *n*-type source in GaN. However, in high resistivity and *p*-type samples, nitrogen vacancies can be a compensating defect.

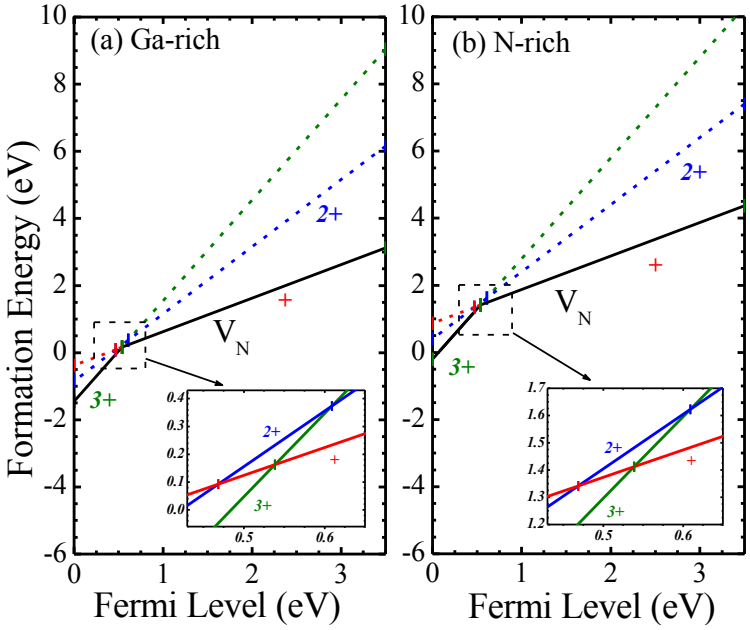

FIG. 7. Formation energies of the V_N defect in GaN grown under (a) Ga-rich and (b) N-rich conditions. The dashed lines are used to emphasize the presence of negative-*U* behavior where

$U = -0.13$ eV. The insets show the regions with the 2+/+ and 3+/2+ transition levels located at 0.47 eV and 0.61 eV above the VBM, respectively.

A nitrogen vacancy in GaN introduces two nearly degenerate localized defect states within the electronic bandgap, and a weakly localized shallow donor state, which is too shallow to be accurately described in our supercell calculations. The charge density of one of the nearly degenerate localized defect states (computed in 3+ charge state of V_N) is displayed in Figure 8. This defect state is a *spd*-hybridized orbital. The charge density strongly localized at the vacancy site consists of mostly *s*-character. The defect state also spreads to nearest Ga atoms (where it has 10% *s*-, 70% *p*-, and 20% *d*-character) and next nearest N atoms (80% *p*- and 20% *s*-character). The degeneracy of the two defect states along with large lattice relaxation causes the negative-*U* behavior of V_N. In the singly positive charge state, the Ga nearest neighbor along the *c*-axis relaxes away from the N vacant site by 2.15%, while the remaining three Ga neighbors also undergo an outward relaxation of 1.60%, compared to ideal Ga-N bond length. In the +3 charge state (Fig. 8), the breathing relaxation is much larger, where the neighboring Ga atom moves away from the N vacant site by 22.1% (Ga atom along the *c*-axis) and 19.5% (atoms in Ga plane).

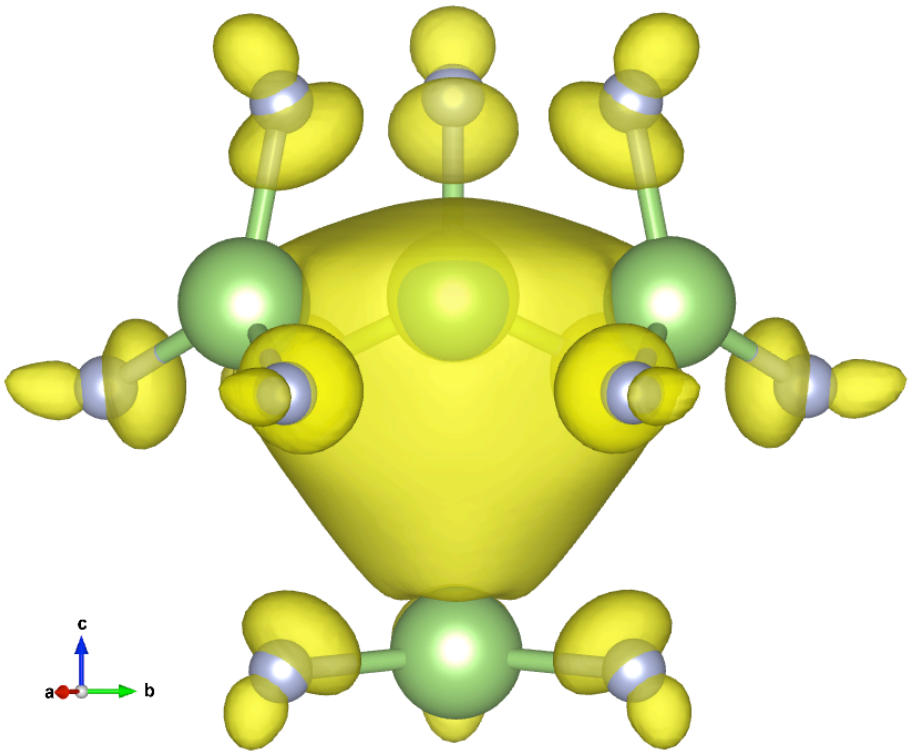

FIG. 8. Charge density of the localized defect state of V_N calculated in the 3+ charge state. The isosurfaces with the value 6 % of the maximum are shown. There is a strongly localized charge density at the vacancy site, which is of *s*-character, while *s*- and *p*-hybridized parts of the defect state are formed at the neighboring N sites.

A detailed experimental and theoretical analysis of the optical properties of V_N in bulk GaN has been previously published in Ref. [20]; here we briefly outline them to present a complete picture of native defects in GaN. The optical transition through the V_N 2+/+ level is internal, as previously suggested.[20] Initially, a positive V_N^+ ground state cannot efficiently trap a photogenerated hole, instead it traps an electron at the shallow +/0 level, making the defect overall neutral. It then traps a hole at a deep 2+/+ level, transferring the V_N into excited + charge state. The optical transition due to the recombination of the weakly localized electron at the

shallow +/0 level and a hole localized at the 2+/+ level has a calculated energy of 2.24 eV. The Frank-Condon shift (relaxation energy) of the + charge state following this transition is 0.78 eV, yielding a ZPL of 3.02 eV. The CCD (Fig. 9) fitted into the calculated optical transitions show that the resonant excitation energy is 0.77 eV below the energy of the crossover of the parabolas. The barrier for the thermal jump via this crossover from the vibrational ground state is 1.53 eV. This makes nitrogen vacancy most likely a radiative defect via the +/2+ transition level. The calculated optical transitions are in good agreement with the experimentally measured GL2,[20] i.e. PL maximum of 2.35 eV, and estimated ZPL in the range of 2.85-3.0 eV. The assumption that the GL2 band is caused by an internal transition between the excited and ground states of V_N^+, is supported by the experimentally observed exponential decay of the GL2 emission after pulsed excitation at low temperature, and invariance of the GL2 band's shape and position with changing excitation intensity.[20]

HSE calculations of optical transitions of V_N in *p*-type GaN, via the 3+/2+ level, can also be performed, where the emission line is computed to be 2.09 eV and the ZPL at 2.88 eV.[20] However, no experimental PL band for such transition has been observed.

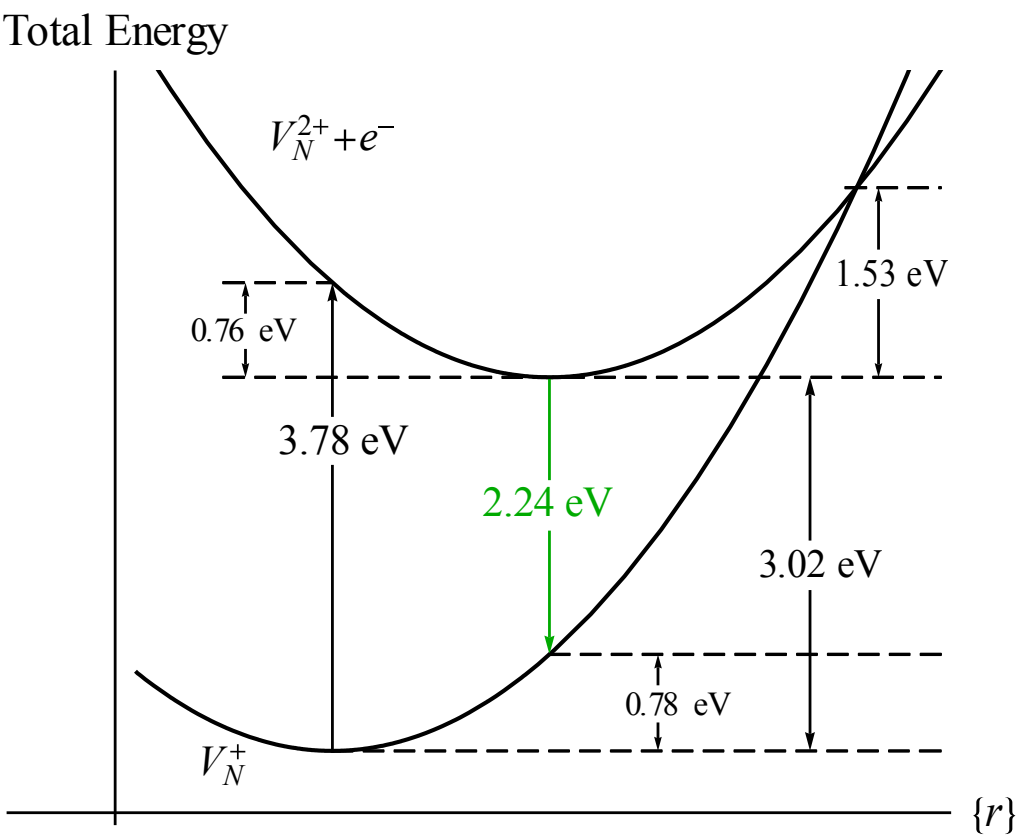

FIG. 9. Configuration coordinate diagram of optical transitions for V_N. The PL maximum is 2.24 eV. Here the vibrational ground state of V_N^{2+} is 1.53 eV lower than the energy of the crossover of the potential curves, which makes transitions via the +/2+ level of V_N most likely radiative. The Franck–Condon shift of V_N^+ is computed to be 0.78 eV and the ZPL is 3.02 eV. These parameters are in close agreement with experimentally observed GL2 band.

Ga-N divacancy ($V_{Ga}V_N$)

The relatively low formation energies of both V_{Ga} and V_N in *n*-type and *p*-type GaN, respectively, prompt the question of whether the isolated vacancies could bind into a stable complex ($V_{Ga}V_N$) divacancy. Figure 10 (a) displays the formation energies of the divacancy in its most stable charge states, i.e, 3+, +, 0, -, and 2-. The divacancy behaves as a deep donor as well as a deep acceptor, with calculated transition levels 3+/2+, 2+/+, +/0, 0/- and -/2- occurring at 0.81 eV, 0.68 eV, 0.98 eV, 1.48 eV and 1.95 eV above the VBM, respectively. The lack of stability of the 2+ charge state, being a characteristic of a negative-*U* defect, is a result of large charge-dependent atomic relaxations around the divacancy. In the 3+ charge state, the nearest N atoms around the vacant Ga site relax away by 11.7%, while the neighboring Ga atoms around the vacant N site move outwardly by 19.3%, compared to bulk Ga-N bonds. The 2- charge state is associated with smaller breathing relaxations around the empty Ga site (5.95 %) and vacant N site (5.33 %). According to Fig. 10 (a), divacancies ($V_{Ga}V_N$) display relatively low formation energies for Fermi levels close to the CBM. Note that the formation energy of the complex is comparable to that of V_{Ga} ($\Delta E_f \sim 0.08$eV) in *n*-type GaN, making it the second most probable intrinsic defect to occur in *n*-type GaN. In addition to the divacancy being fairly favorable in *n*-type GaN, it also displays a significantly large binding energy of 3.04 eV (Fig. 10 (b)) for Fermi levels above 2.34 eV from the VBM. In *p*-type GaN, the divacancy exhibits a binding energy of ~1 eV. Hence, divacancies are expected to be stable in bulk GaN if they are formed during growth or as a result of the electron irradiation. The stability of divacancies in *n*-type GaN was also suggested in Refs. [27, 34]; however no definite experimental identification of divacancies in *n*-type GaN has been demonstrated to date.

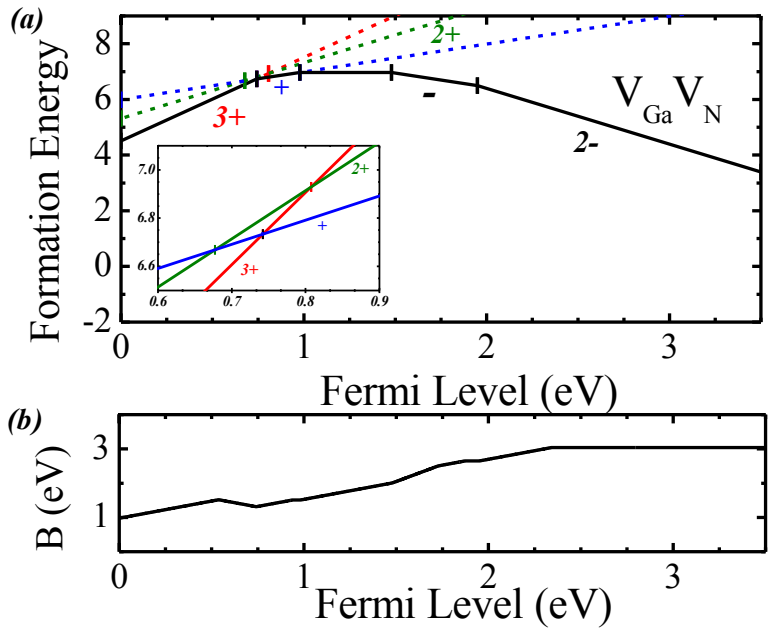

FIG. 10. (a) Formation energy of the most stable charge states of the $V_{Ga}V_N$ defect (solid black line), in GaN grown under either Ga- or N-rich conditions. The dashed lines display the instability of the 2+ charge state or the negative-U behavior ($U = -0.13$ eV). The insets show the 2+/+ and 3+/2+ transition levels occurring at 0.68 eV and 0.81 eV, above the VBM, respectively. (b) Binding energy (B) of $V_{Ga}V_N$ as a function of the Fermi level across the band gap. In *n*-type GaN, the binding energy is calculated to be 3.04 eV.

Figure 11 displays the CCD obtained by parabolic fits into the calculated optical transitions of divacancy via the 2-/- transition level. Starting from $V_{Ga}V_N^{2-}$ as the ground state in typical *n*-type GaN, the resonant excitation energy is predicted at 2.00 eV. A negatively charged $V_{Ga}V_N^{2-}$ captures a free hole at the 2-/- level. If radiative, the subsequent recombination of an electron in the conduction band (or bound to a shallow donor) and the hole localized at $V_{Ga}V_N^{-}$, has a calculated energy of 0.99 eV, with a Franck–Condon shift of 0.54 eV, and a ZPL of 1.53

eV. The calculated 0.99 eV emission peak is very close to the maximum of the experimentally observed broad structureless near-IR band (~0.95 eV) in electron irradiated GaN epilayers,[12-17] thus making divacancy a possible candidate for this PL band. However, in the divacancy case, the calculated absorption energy is 0.12 eV larger than the energy of the crossover of the potential curves. The barrier for a non-radiative transition from the vibrational ground state of $V_{Ga}V_N^-$ via this crossover is 0.35 eV. This value of the energy barrier suggests significant temperature dependence of the non-radiative transition probability. Assuming a typical phonon frequency of 10^{13} s^{-1} and following Ref. [28], an estimation of the thermal jump probability suggests that at room temperature this defect is likely non-radiative. However, depending on the radiative lifetime of the PL, (the time the defect remains in the excited state), at a certain low temperature, the radiative recombination should prevail. Estimating this temperature requires the knowledge of the PL lifetime. This is in reasonable agreement with recent experimental studies of electron-irradiated GaN samples where appearance of the broad 0.95 eV PL band at low temperature (4.2 K) was observed and its near disappearance (~85%) after room temperature annealing (295 K) occurred.[17]

An alternative explanation of 0.95 eV near-IR band has been discussed based on experiments (Refs. [15-17]). It was suggested that the migration of interstitial Ga (Ga_i defects are analyzed in Section B) near a vacant Ga site could play an important role in the broad 0.95 eV PL band. We performed HSE calculations of various configurations of defect complexes consisting of Ga_i with neighboring V_{Ga}. However, as a result of relaxation, interstitial Ga relocates into the vacancy making the complex $V_{Ga}Ga_i$ unstable. Therefore, if electron irradiation creates Ga_i in the immediate vicinity of V_{Ga}, the resulting complex quickly annihilates. In addition to $V_{Ga}Ga_i$,

several atomic configurations of the complex Ga_NV_{Ga} were investigated. However, upon relaxation, Ga antisite also relocates into the Ga vacancy, yielding the isolated nitrogen vacancy.

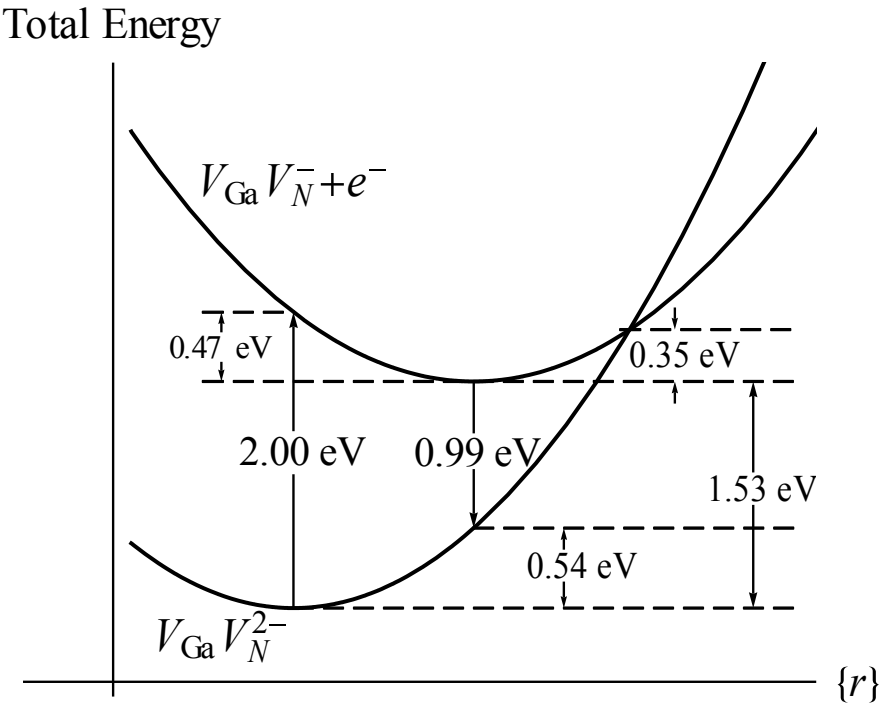

FIG. 11. Configuration coordinate diagram for the optical transitions via $V_{Ga}V_N$ defect in GaN. The emission is predicted to occur at 0.99 eV while the FC shift and ZPL are calculated to be 0.54 eV and 1.53 eV, respectively. Here the vibrational ground state of $V_{Ga}V_N^-$ is 0.35 eV below the energy of the crossover of the potential curves, suggesting that this defect is radiative only at low temperatures.

B. Gallium Defects

Interstitial Ga (Ga_i)

HSE calculations show that interstitial Ga occurs in the +, 2+ and 3+ charge states and its most stable configuration is a near octahedral site, which is in agreement with recent HSE results.[39,40] Interstitial Ga at the tetrahedral site is found to be 93 meV higher in energy than a near octahedral Ga_i. Figure 12. (a) displays the ideal atomic configurations of the tetrahedral and octahedral interstitial sites in the primitive wurtzite GaN unit cell. For comparison, the relaxed geometry of Ga_i in the + charge state is shown in Fig. 12. (b). In a singly positive charge state (+), the distances from interstitial Ga to the two neighboring Ga planes are 2.52 Å and 2.39 Å, and the distances between Ga_i and N atoms in the two nearest N planes are 2.00 Å and 2.75 Å. In the 3+ charge state, when compared to the corresponding bonds of Ga_i^+, the Ga_i-Ga bonds exhibit slight outward breathing relaxation of 3.38% and 0.89%, respectively, while the Ga_i-N distances decrease by 1.76% and 12.2%. The attraction between interstitial Ga and nearest N atoms in the 3+ charge state obtained from HSE calculations also agrees well with previous DFT results.[28]

The formation energies and transition levels of interstitial Ga are shown in Fig. 13. This defect forms two deep donor transition levels 3+/2+ and 2+/+ at 2.33 eV and 2.64 eV, above the VBM, respectively. The +/0 transition level is found to be resonant with the CBM, suggesting the existence of a shallow donor state inaccessible in our supercell calculations. In both growing environments, for Fermi level values close to the VBM, Ga_i is the most energetically favorable defect among substitutional and interstitial native defects (i.e. excluding vacancies). Since Ga_i is a donor defect, it could therefore act as compensating center for *p*-type GaN. On the other hand,

interstitial Ga has high formation energy for Fermi levels near the CBM, suggesting that it is unlikely to form in *n*-type GaN.

Our calculations of the interstitial Ga can help explain the nature of the sharp near-IR band observed in 2.5 MeV electron-irradiated GaN samples. This PL band peaks at 0.85 eV, and has a zero phonon line (ZPL) at 0.88 eV. Based on the slight shift of the peak of this PL band observed in different GaN epilayers, Buyanova et al.[13,67] argued that it could be caused by an internal transition between the excited state close to the CBM and the ground state of a deep isolated defect. Further experimental study on this PL band performed by Chen et al.[68] suggested that the sharp near IR PL peak is related to either isolated substitutional O_N impurity (which is unexpected since O_N is known to be a shallow donor) or a complex associated with O_N. Overall, to our knowledge, no conclusive experimental or theoretical explanation of the microscopic origin of the sharp 0.85 PL band in electron-irradiated GaN has been provided thus far. Our HSE calculations suggest that an internal transition between the excited and ground state of the + charge state of the interstitial Ga is responsible for this PL band.[12-17,67]

For Fermi levels close to the CBM, interstitial Ga has the lowest energy in the + charge state (Fig. 13). As mentioned above, in our calculations, the +/0 transition level is resonant with the conduction band, which implies a shallow donor level likely a few tens of meV below the CBM. At low temperatures and under the ultraviolet (UV) illumination, generating an electron-hole pair, the unoccupied shallow donor level of Ga_i^+ can capture the electron, transferring the defect into neutral charge state Ga_i^0. Since the captured electron is weakly localized on Ga_i, almost no relaxation of the lattice occurs. Subsequently a free hole from the VBM is captured by the neutral defect at the 2+/+ transition level. Since this defect state is strongly localized, the hole capture leads to the lattice relaxation, which corresponds to the minimum energy lattice of Ga_i^{2+}.

Consequently, the defect is now converted into Ga_i^{2+} plus a weakly localized electron. Finally, an internal transition occurs, i.e. the recombination of the weakly localized electron from the shallow +/0 level and a hole strongly localized at the 2+/+ deep defect level. We calculate the energy of this transition to be 0.72 eV, which should cause a near IR PL band. The obtained relaxation energy (Franck-Condon shift) following this transition is 0.12 eV, yielding a ZPL of 0.84 eV, suggesting that this transition produces a sharp PL band.

The calculated CCD and the optical transitions via interstitial Ga are displayed in Fig. 14. In this case, the potential curves are found to never intersect, hence the path for non-radiative transitions described above in section III. A is unavailable. This defect is therefore likely to be radiative. Our calculated optical transitions (shown in Fig. 14) for interstitial Ga are in good agreement with the previously observed 0.85 eV PL band associated with a sharp ZPL of 0.88 eV in electron-irradiated GaN samples.[12-17,67] Most recent HSE calculations of the migration mechanisms of interstitial Ga in the + charge state show a diffusion energy barrier of 1.6 eV.[40] In *n*-type GaN, Ga_i occurs in the + charge state (Fig. 13). Using the approximation for thermal jump rate (discussed in the section I.C. *Ga-N divacancies*), it can be estimated that Ga_i become mobile at temperatures around 620 K.

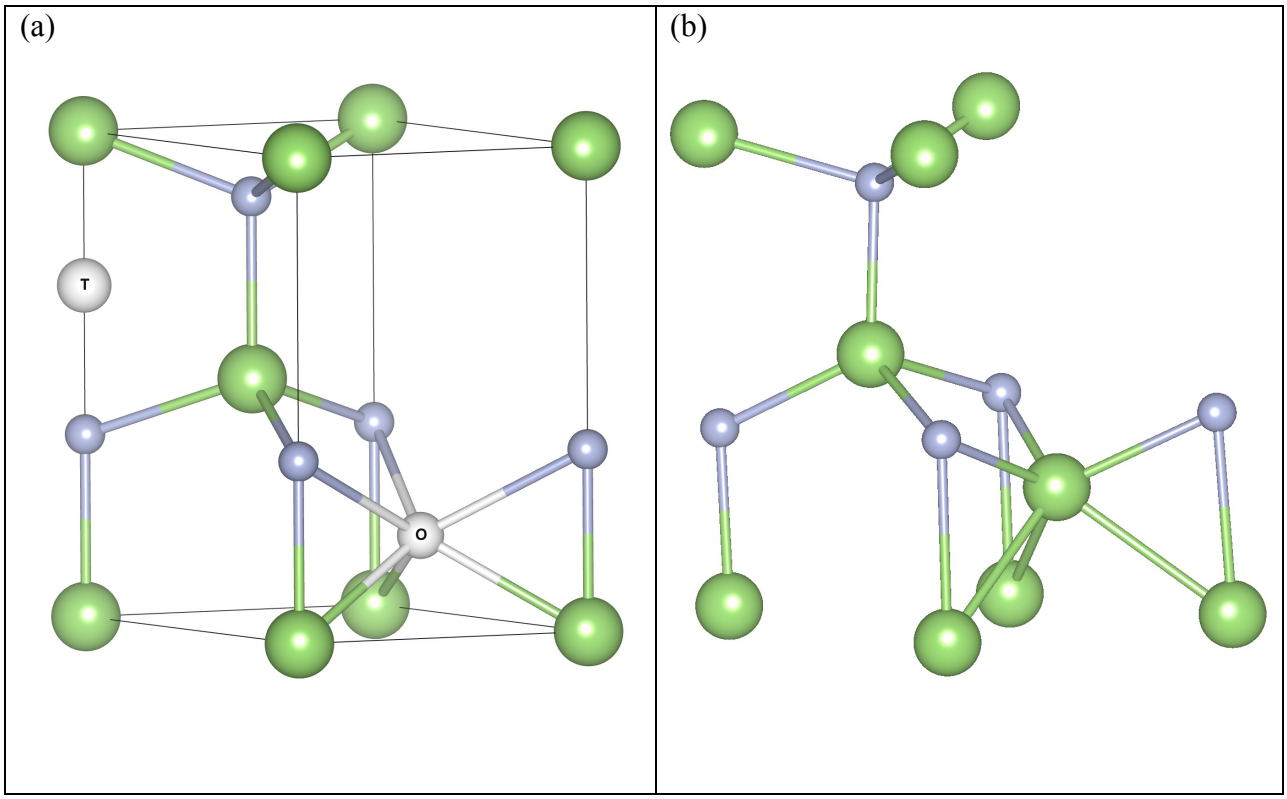

FIG. 12. (a) Atomic configuration of the tetrahedral (labeled T) and octahedral (labeled O) interstitial sites in the wurtzite GaN. Large green spheres represent Ga atoms and small grey spheres represent N atoms. (b) Relaxed atomic structure of Ga_i in the + charge state. The Ga atom occupies a slightly distorted octahedral site, where the distances between Ga_i and nearest N atoms decrease by 4.28%, when compared to ideal octahedral configuration.

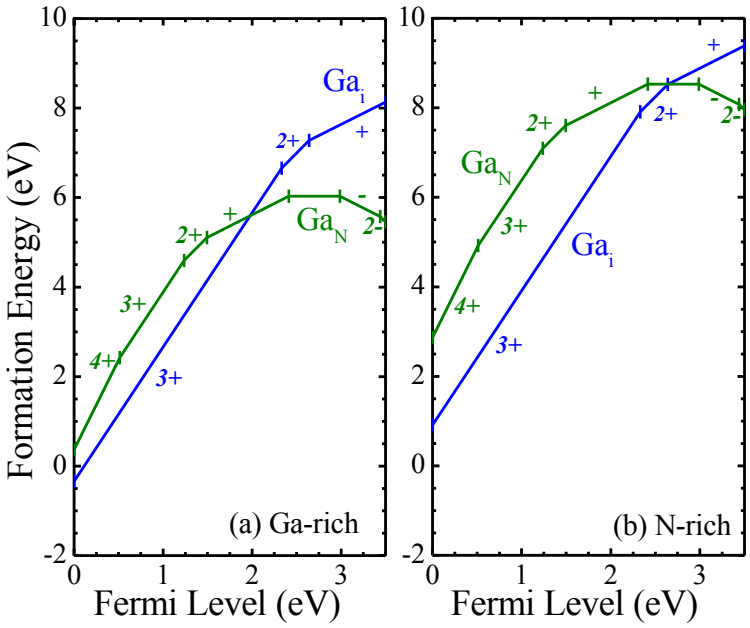

FIG. 13. Formation energies of the Ga native defects as a function of the Fermi energy calculated for (a) Ga-rich and (b) N-rich growth conditions. In *p*-type GaN and Ga-rich environment, both interstitial and antisite Ga possess the lowest formation energies among investigated substitutional and interstitial native defects, while displaying very high formation energies in *n*-type GaN in both growth conditions.

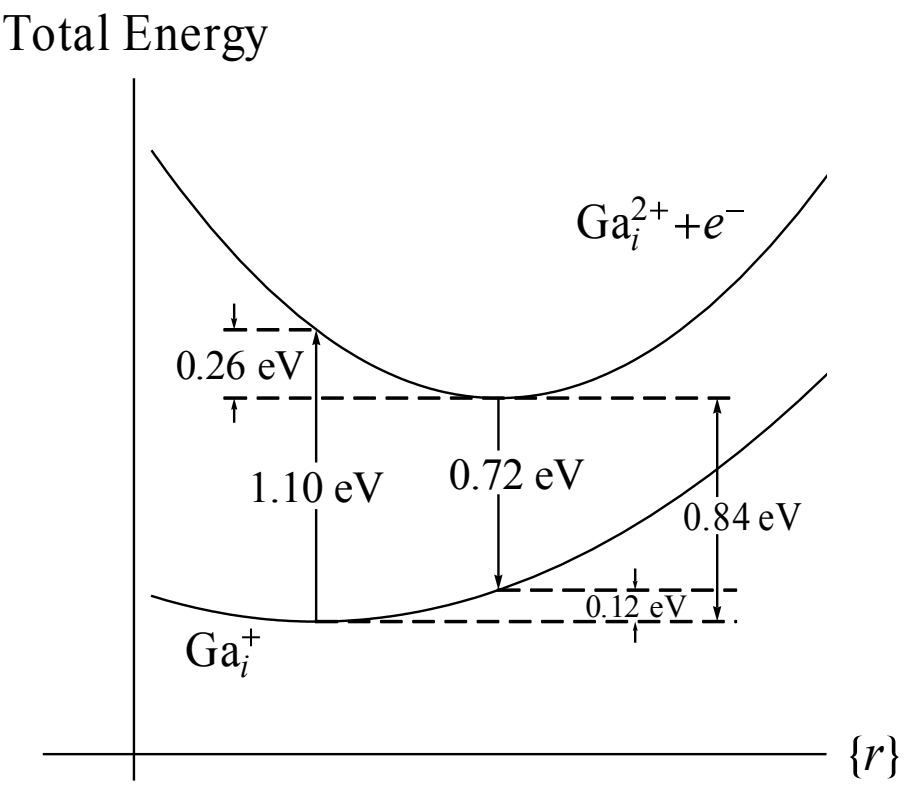

FIG. 14. Configuration coordinate diagram for the isolated interstitial Ga, displaying calculated optical transitions via the +/2+ transition level. The peak of the PL band is at 0.72 eV. The two potential curves never intersect, making Ga_i likely a radiative defect. The ZPL is found to be 0.84 eV and the Franck-Condon shift (relaxation energy) is 0.12 eV.

Gallium antisite (Ga_N)

HSE calculations show that Ga antisite exhibits multiple stable charge states, depending on the Fermi level within the gap, i.e, 4+, 3+, 2+, +, 0, - and 2-. The 4+ charge state is associated with considerable atomic distortions where the antisite defect relaxes along the *c*-axis which consequently pushes away its *c*-axis neighboring Ga atom by ~0.50 Å from its initial site. As a result, the Ga_N-Ga bond parallel to the *c*-axis is 36.8% longer than the ideal bulk Ga-N bond length. The three remaining Ga_N-Ga bonds are 24.3% longer. In contrast, in the 2- state, the Ga_N-Ga bonds undergo weaker outward relaxations of 11.1% and 10.3%, respectively.

Figure 13 displays the formation energy as a function of the Fermi level for Ga antisite in GaN grown under (a) Ga-rich and (b) N-rich conditions. Ga antisite behaves as a donor and an acceptor defect and exhibits six transition levels within the bandgap. The 4+/3+ occurs at 0.52 eV, 3+/2+ at 1.24 eV, 2+/+ at 1.50 eV, +/0 at 2.42 eV, 0/- at 2.99 eV and -/2- at 3.44 eV, above the VBM. Note that the -/2- transition level is very close to the CBM (~0.06 eV), making it difficult to confirm the stability of the 2- charge state. In Ga-rich conditions and for Fermi level close to the CBM, Ga antisites display formation energies lower to that of interstitial Ga ($\Delta E_f \sim 2.67\,\text{eV}$), whereas in *p*-type GaN, Ga_N is less energetically favorable than Ga_i by $\sim 0.7\,\text{eV}$.

C. Nitrogen Defects

Interstitial Nitrogen

As possible interstitial configurations of N in wurtzite GaN, we consider two distinct hexagonal sites ($N_{Hex\text{-}Ga}$ and $N_{Hex\text{-}N}$), the channel-centered site[69] (N_{CC}), the two octahedral sites (N_O), and the split interstitial geometry (N_i-N_i). The two interstitial hexagonal configurations, $N_{Hex\text{-}Ga}$ and $N_{Hex\text{-}N}$, are located at the centers of the Ga and N triangles in hexagonal planes, respectively. The channel-centered site (N_{CC}) is located at the center of the hexagonal channel between the two adjacent Ga and N planes. The two N_O sites are octahedrally coordinated by Ga and N atoms respectively, and located symmetrically at ~0.32 Å away from the N_{CC} cite along the wurtzite *c*-axis. Finally, the split-interstitial site corresponds to the two neighboring N atoms sharing the same N site as shown in Fig.15(b, c), compared to ideal GaN lattice (Fig.15(a)).

Neutral interstitial N in the channel-centered site $\left(N_{CC}^{0}\right)$ is slightly distorted as a result of relaxation. Interstitial N atom moves along the wurtzite *c*-axis into a site located at about 2.10 Å and 2.22 Å from the Ga and N planes, respectively. Both neutral octahedral interstitial N sites are unstable, and the N atom relaxes into the above mentioned near channel-centered site. Similarly, nitrogen interstitial in the hexagonal site ($N_{Hex\text{-}Ga}$) is unstable, and upon relaxation, the N atom also relocates to the near channel-centered site (N_{CC}). The other hexagonal geometry $N_{Hex\text{-}N}$ in the neutral state is also distorted, i.e. the N atom is pushed away by one of three adjacent N atoms toward the other two by ~0.2 Å within the same nitrogen layer.

Our HSE calculations show that among all investigated interstitial N sites, the most stable configuration is the split-interstitial geometry (Fig. 15(b, c)). This defect was recently observed using high frequency EPR and electron nuclear double resonance (ENDOR) measurements in

irradiated *n*-type GaN.[70] In the calculations, the initial N_i-N_i bond distance was chosen to be 1.13 Å, which is comparable to the bond distance of ideal N_2 molecule (1.1 Å).[28] N split interstitial defect exhibits multiple charge states, 3+, 2+, +, 0 and -. The relaxed atomic structures of the singly negative (-) and 3+ charge states of split interstitial N are displayed in Figs. 1(b) and 1(c). In the negative charge state, the N_i-N_i bond length is 1.41 Å while the distances from the N_i atoms to their nearest Ga atoms decrease by 7.48% and 6.82%, respectively, when compared to corresponding ideal Ga-N bonds. In the 3+ charge state, the N_i-N_i bond length is 1.11 Å and the N_i-Ga bonds undergo outward breathing relaxations of 29.7% and 17.4%, respectively. After relaxation, N split interstitial defect has formation energy that is 2.58 eV and 2.97 eV lower than those obtained in the $N_{Hex\text{-}N}$ and the near channel-centered sites, respectively. The obtained large differences in formation energies are also in good agreement with previous DFT calculations.[24,28]

Figure 16 shows calculated formation energies of the N split interstitial (N_i-N_i) as a function of the Fermi energy in Ga- and N-rich growth conditions. N split interstitial displays both acceptor 0/- transition level at 0.48 eV below the CBM, and several deep donor levels, namely, the +/0, 2+/+ and 3+/2+, respectively occurring at 2.45 eV, 0.51 eV and 0.22 eV above the VBM. Overall, nitrogen interstitial defect has relatively low formation energy, compared to other interstitial and antisite defects in GaN.

In addition to N split interstitial, the possible incorporation of the nitrogen molecule (N_2) into the GaN lattice was investigated. The N_2 molecule was placed at the center of the hexagonal cage in various directions relative to the *c*-axis and at the Ga-N bond center. HSE calculations of the various relaxed configurations of N_2 yield formation energies that are significantly higher than that obtained for the N split interstitial ($\Delta E_f \geq 4.81$ eV), hence making the interstitial N_2 molecules incorporation into bulk GaN unlikely.

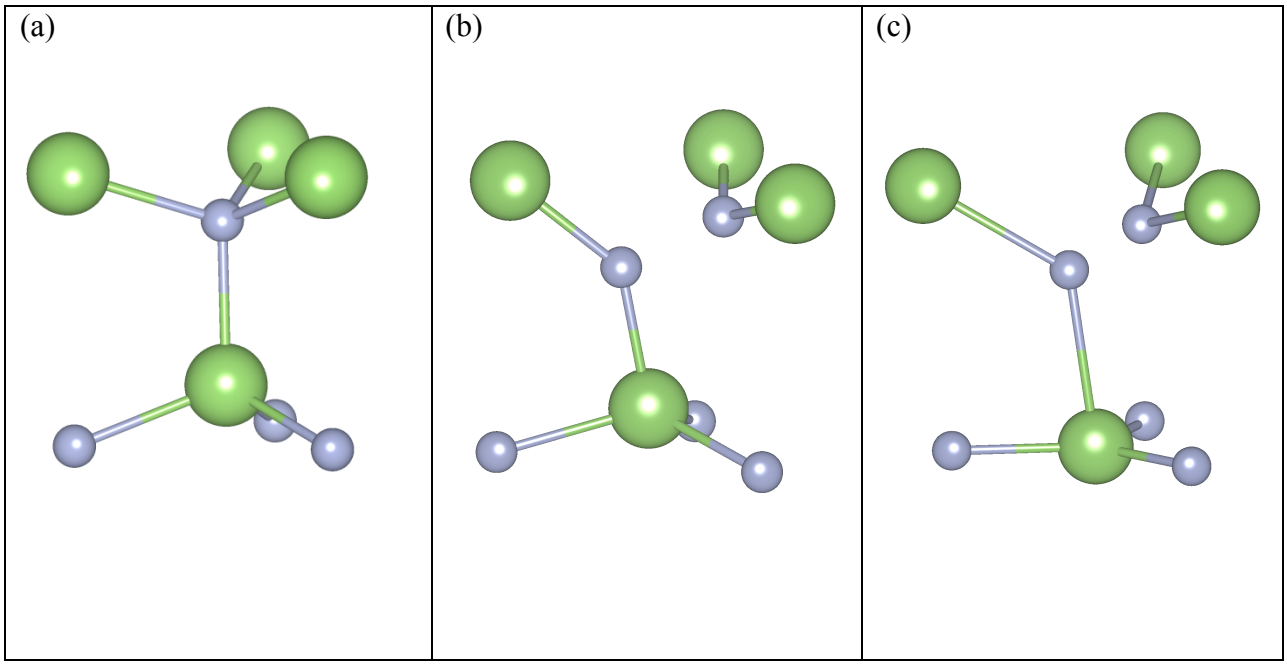

FIG. 15 (a) Atomic structure of the section of ideal wurtzite GaN; (b) equivalent section of the relaxed N split interstitial (N_i-N_i) in the singly negative (-) charge state and (c) in the 3+ charge state. Large green spheres represent Ga atoms and small grey spheres represent N atoms. In the - charge state, the N_i-N_i bond is 1.41 Å; in the 3+ charge state, the N_i-N_i bond is reduced to 1.11 Å.

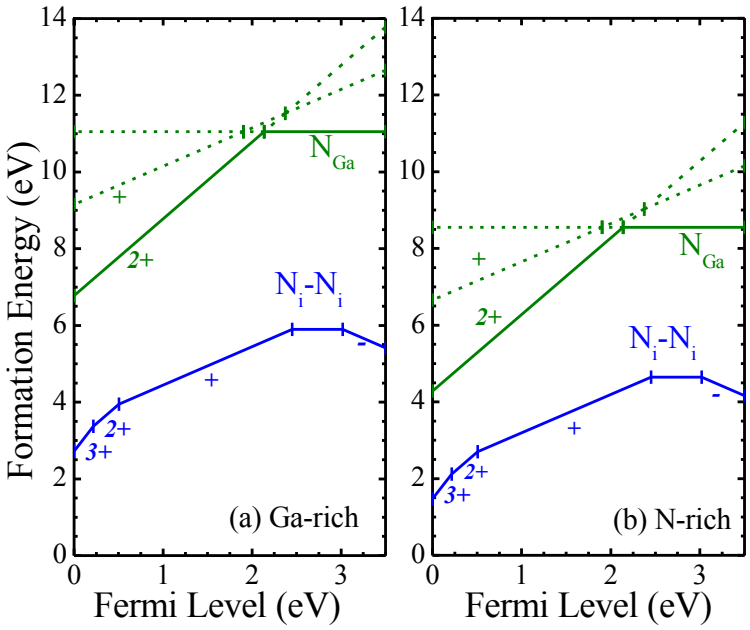

FIG. 16. Formation energies of native nitrogen defects as a function of the Fermi energy for GaN grown in (a) Ga-rich and (b) N-rich environments. The dashed lines are used to show the instability of the + charge state for the N antisite, displaying a negative-U character ($U = -0.73$ eV).

Nitrogen Antisite (N_{Ga})

The formation energies of N antisite (N_{Ga}) are shown in Fig. 16(a) and (b). N antisite is a deep donor, stable in the 2+ charge state for Fermi levels below ~2.40 eV from the VBM, and in the neutral state above that value. In the neutral charge state, the distance between N antisite and its three nearest N atoms decrease by 6.3 %, compared to bulk Ga-N bond length. The 2+ charge state of N_{Ga} is associated with substantial inward relaxation of 23.9% of N_{Ga}-N bonds, where the neighboring N atoms relax towards N antisite. Note that the + charge state is higher than both 2+ and 0 charge states; this is a characteristic of a negative-*U* defect, which is associated with large lattice relaxations in 2+ charge state. Among all possible native defects investigated in this paper, N_{Ga} possesses the highest formation energy in both growing environments, and in both *n*-type and *p*-type GaN. Such high formation energy implies that N_{Ga} defects are unlikely to form.

Summary of thermodynamic transition levels $\varepsilon(q_1/q_2)$ of native defects in GaN

TABLE I. Thermodynamic transition levels $\varepsilon(q_1/q_2)$ of all investigated native defects in GaN, with the reference to the VBM, and their comparison with previous theoretical works.

Defects	q_1/q_2	$\epsilon(q_1/q_2)$ in eV Present work	$\epsilon(q_1/q_2)$ in eV HSE	$\epsilon(q_1/q_2)$ in eV sX-LDA	$\epsilon(q_1/q_2)$ in eV LDA and PBE-GGA
V_{Ga}	+/0	0.94	0.82[g]; 0.97[d]	…	…
	0/-	1.73	1.63[g]; 1.88[b]; 1.68[d]	1.37[e]	0.25[a]
	-/2-	1.87	2.09[g]; 2.10[b]; 2.33[d]	1.88[e]	0.64[a]
	3-/2-	2.34	2.3-2.4[g]; 3.13[b]; 2.80[d]	2.09[e]	1.10[a]
V_N	3+/2+	0.61	…	…	…
	3+/+**	0.54	0.50[g]; 0.68[b]; 0.47[f]; 0.70[i]	0.68[e]	1.18[a]
	2+/+	0.47	…	…	…
	+/0	CBM*	3.21[g]; 3.17[b]; 3.26[f]	…	…
	+/-**	…	…	3.32[e]	…
	0/-	…	3.4[g]		
$V_{Ga}V_N$	3+/2+	0.81	…	…	…
	3+/+**	0.74	…	…	…
	2+/+	0.68	…	…	0.5[c]
	+/0	0.98	…	…	0.65[c]
	0/-	1.48	…	…	…

	0/2-**	…	…	…	~0.66-0.7[c]
	-/2-	1.95	…	…	…
Ga_i	3+/2+	2.33	2.18[g]; 2.43[b]	…	2.55[a]
	2+/+	2.64	2.42[g]; 2.83[b]	…	2.39[a]
	+/0	CBM*	…	…	…
Ga_N	4+/3+	0.52	1.56[b]	…	0.93[h]
	3+/2+	1.24	1.60[b]	…	1.86[h]
	2+/+	1.50	2.13[b]	…	2.08[h]
	+/0	2.42	2.50[b]	…	2.27[h]
	0/-	2.99	3.23[b]	…	2.70[h]
	-/2-	3.44	…	…	…
N_i	3+/2+	0.22	VBM[ǂ(g)]; 0.77[b]	…	0.74[a]
	2+/+	0.51	0.50[g]; 1.80[b]	…	0.90[a]
	+/0	2.45	2.16[g]; 2.20[b]	…	1.48[a]
	0/-	3.02	2.82[g]; 3.28[b]	…	2.00[a]
N_{Ga}	2+/+	2.76	1.70[b]	…	0.88[h]
	+/0	2.03	2.67[b]	…	1.68[h]
	2+/0**	2.40	…	…	…
	0/-	…	…	…	2.70[h]

*: Shallow transition level resonant with the CBM.

**: Crossover due to $-U$ behavior.

ǂ: Transition level resonant with the VBM.

[a] Reference 28.

[b] Reference 39.

[c] Reference 34.

[d] Reference 38.

[e] Reference 37 with Freysoldt corrections.[71,72]

[f] Reference 36.

[g] Reference 40.

[h] Reference 26.

[i] Reference 56.

Transition levels of all investigated intrinsic defects in this paper are shown in Fig. 17. Also, a comparison between defect transition levels obtained here and in previous theoretical works is displayed in Table I.

In the case of V_{Ga}, the absence of the +/0 transition level in Ref. [28] (using LDA) and Ref. [37] (using sX-LDA), and the differences in other transition energies could be attributed to the use of different exchange-correlation functionals in these works. The application of different functionals can also lead to different atomic relaxations of the nearest N atoms around the vacant Ga site. For example, in the 3- charge state, our HSE calculations yield an outward breathing relaxation of ~9-10%, which is approximately twice of that previously obtained with LDA (4%).[28] The differences in lattice relaxations of a defect also contribute to the discrepancies in calculated transition levels. However, our calculated relaxations of nearest N atoms around V_{Ga}^{3-} are similar to the 11-12% relaxation values obtained by sX-LDA in Ref. [37], while the resulting 2-/3- transition levels differ by 0.25 eV. Therefore the difference in defect relaxations in different methods is not the only contributing factor in the transition level discrepancies.

The transition levels for vacancy of Ga described in this paper mostly agree with most recent HSE calculations (see Table I). However, Ga vacancy transition levels 2-/3- and -/2- obtained in Refs. [38, 39], were found to occur deeper with respect to VBM in the band gap.

Although the Ga 3*d* electrons were used in those calculations, our tests show that the inclusion of Ga 3*d* electrons results in negligible differences for calculated transition levels. Other possible sources of the discrepancies are the **k**-point sampling methods and supercell sizes. For example, in Ref. [38], using a 2×2×2 **k**-point mesh and 96-atom supercells, a formation energy of 4.42 eV (calculated at CBM) was obtained for V_{Ga}^{3-} which is 1.10 eV higher than our obtained values of 3.32 eV (calculated at **Γ**-point in 128-atom hexagonal supercell). In Ref. [39], HSE calculation with an off-center single **k**-point and 108 atom-supercells, an energy of 3.2 eV (at CBM) was obtained for V_{Ga}^{3-} which only differs from our result by 0.1 eV. Our tests also show that using the above **k**-point sampling methods produces formation energy differences of ~0.05 eV.

Finally, the difference in the results could be due to the use of different electrostatic correction schemes. Two common approaches are the Freysoldt corrections[71,72], used in Refs. [38-40], and the Lany and Zunger corrections[43] used in this paper. As could be seen from Table I, our results tend to be similar to HSE results of Refs. [38, 39] for transition levels between the low charge states, and significantly different for high charge state transition levels. However, the discrepancies between our results and the results from Ref. [40] tend to be small even for high charge state transition levels (in the latter work, a slightly smaller amount of exact exchange of 29% was used).

For the nitrogen vacancy, the crossover 3+/+ (negative-*U* center) is also similar in most recent HSE calculations.[36,40] Nevertheless, in contrast to this work, the shallow +/0 transition level was not obtained, rather a +/0 level was predicted to be deep, occurring at 0.15-0.2 eV below the CBM.[36,39,40]

Although the negative-*U* character of divacancies was also described in Ref. [34] using GGA, authors obtained a 0/2- crossover at ~0.66-0.7 eV above the VBM, while we obtain a 3+/+ crossover at 0.74 eV. The formation energy calculated in Ref. [34] for the divacancy in the 2- charge state is ~1.2 eV lower than in this work.

Previous LDA predictions of negative-*U* center of interstitial Ga are not reproduced in this paper.[26,28] The atomic relaxations obtained here are very similar to previous LDA results for interstitial Ga in the 2+ charge state. The use of the LDA functional in Refs. [26, 28] is the source of the transition levels discrepancies. Recent HSE calculations[39] of Ga_i show a difference in transition levels of the 3+/2+ and 2+/+ of 0.1 eV and 0.2 eV, in the + and 3+ charge states, respectively, when compared to our work. Here, we also notice that the differences are not following the charge states of the defects. Comparison of transition levels of antisite defects (Ga_N and N_{Ga}) and N split interstitial with previous HSE results show similar trends as previously discussed.

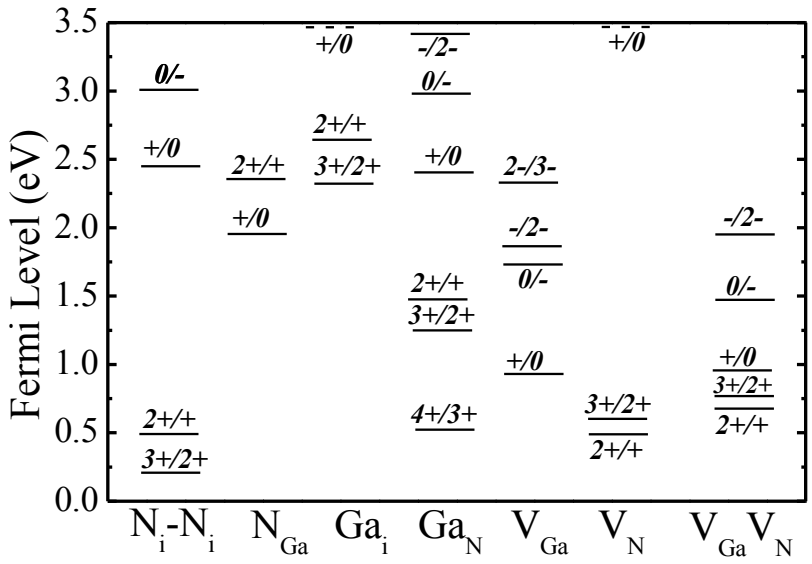

FIG. 17. Thermodynamic transition levels $\varepsilon(q_1/q_2)$ of all investigated native defects in GaN, with the reference to the VBM. The solid lines denote the positions of the deep defect transition levels. The +/0 transition levels of Ga_i and V_N are calculated to be resonant with the conduction band, which suggests that experimentally, shallow donor levels (dashed lines) of these defects should be observed.

IV. CONCLUSIONS

We have performed theoretical investigation of the electronic and optical properties of native defects in GaN. The use of exchange tuned HSE leads to significant changes in the predictions of thermodynamic transition levels and optical transitions for several intrinsic defects in GaN compared to local approximations to the DFT. The differences can be attributed to the improved treatment of electronic interactions forming defect levels. In this paper, we have considered most common native defects, i.e, V_{Ga}, V_N, $V_{Ga}V_{N,}$ Ga_i, Ga_N, N_i-N_i, N_{Ga}, Ga_iV_{Ga} and Ga_NV_{Ga}. We estimate the likelihood of radiative versus non-radiative nature of transitions via defects based on the barrier height for the crossover of the potential curves of two different charge states.

Analysis of the configuration coordinate diagram constructed from the computed HSE transition energies suggests that Ga vacancy is likely a non-radiative defect. Our calculations of Ga vacancy show that V_{Ga} in the neutral state exhibits a large magnetic moment of 3 μ_B, while in the + charge state, the spins on the four neighboring nitrogen atoms around the vacant Ga site favor an AFM order over a FM spin configuration with energy difference of 75 meV.

Nitrogen vacancy is found to be the most energetically stable native defect in *p*-type GaN and for Fermi levels up to ~3 eV above the VBM. Calculated transitions via the 2+/+ level of V_N show an emission occurring at 2.24 eV and a zero phonon line of 3.02 eV, which is in good agreement with recent experimental data on observed GL2 band.[20] The PL band of V_N is predicted to originate from internal transitions between a shallow and a deep level of the same defect. The HSE fitted configuration coordinate diagram suggests that V_N is a radiative defect.

In *n*-type GaN, we show divacancies to be fairly energetically stable with a binding energy of 3.04 eV. We also calculate an optical transition (emission) at 0.99 eV via the 2-/- level

of the divacancy, with ZPL of 1.53 eV. This transition could be related to the near IR broad 0.95 PL band, frequently observed in 2.5 MeV electron irradiated GaN samples.[12-17] The calculations also suggest that the transitions via this defect level are radiative at low temperatures and become non-radiative at room temperature.

Among investigated interstitial and antisite defects, both Ga_i and Ga_N were found to be energetically favorable in *p*-type GaN while split interstitial N_i-N_i exhibits the lowest formation energy in *n*-type GaN. Since calculations predict both a shallow donor level and deep levels of Ga_i, the optical transition via this defect is also suggested to be internal, with an electron weakly localized on the shallow level and a hole localized on a deep level of same defect prior to the recombination. Configuration coordinate diagram fitted into the HSE computed optical transitions and lattice relaxations, suggests that Ga interstitial is a radiative defect. Furthermore, interstitial Ga was found to be a good candidate for a defect responsible for the sharp near-IR 0.85 eV PL band associated with a ZPL at 0.88 eV observed in electron-irradiated GaN epilayers.[12-17,67] Calculations also suggest that N antisites are unlikely to occur in bulk GaN.

ACKNOWLEDGEMENTS

This work was supported by the U.S. National Science Foundation (NSF) under Grant No. DMR-1410125 and by VCU Center for High Performance Computing. The authors would like to thank Michael Reshchikov for helpful discussions.

[1] S. Nakamura, T. Mukai, and M. Senoh, Candela□class high□brightness InGaN/AlGaN double□heterostructure blue□light□emitting diodes, Appl. Phys. Lett. **64**, 1687 (1994).
[2] S. Nakamura, and G. Fasol, *The Blue Laser-Diode—GaN Based Light Emitters and Lasers* (Springer-Verlag, Berlin, 1997).

[3] R. Dahal, J. Li, K. Aryal, J. Y. Lin, and H. X. Jiang, InGaN/GaN multiple quantum well concentrator solar cells, Appl. Phys. Lett. **97**, 073115 (2010).
[4] K. Saarinen, T. Laine, S. Kuisma, J. Nissilã, P. Hautojãrvi, L.Dobrzynski, J. M. Baranowski, K. Pakula, R. Stepniewski, M.Wojdak, A. Wysmolek, T. Suski, M. Leszczynski, I. Grzegory, and S. Porowski, Observation of native Ga vacancies in GaN by positron annihilation, Phys. Rev. Lett. **79**, 3030 (1997).
[5] K. Saarinen, T. Suski, I. Grzegory, and D. C. Look, Thermal stability of isolated and complexed Ga vacancies in GaN bulk crystals, Phys. Rev. B. **64**, 233201, (2001).
[6] J. Oila, V. Ranki, K. Saarinen, P. Hautojãrvi, J. Likonen, J. M. Baranowski, K. Pakula, M. Leszczynski, and I. Grzegory, Influence of dopants and substrate material on the formation of Ga vacancies in epitaxial GaN layers, Phys. Rev. B **63**, 045205 (2001).
[7] J. Oila, J. Kivioja, V. Ranki, K. Saarinen, D. C. Look, R. J. Molnar, S. S. Park, S. K. Lee, and J. Y. Han, Influence of dopants and substrate material on the formation of Ga vacancies in epitaxial GaN layers, Appl. Phys. Lett. **82**, 3433 (2003).
[8] A. Sedhain, J. Li, J. Y. Lin, and H. X. Jiang, Nature of deep center emissions in GaN, Appl. Phys. Lett. **96**, 151902 (2010).
[9] J. Neugebauer and C. G. Van de Walle, Gallium vacancies and the yellow luminescence in GaN, Appl. Phys. Lett. **69**, 503 (1996).
[10] R. Armitage, W. Hong, Y. Qing, H. Feick, J. Gebauer, E. R. Weber, S.Hautakangas, and K. Saarinen, Contributions from gallium vacancies and carbon-related defects to the "yellow luminescence" in GaN, Appl. Phys. Lett. **82**, 3457 (2003).
[11] F. Reurings and F. Tuomisto, Interplay of Ga vacancies, C impurities, and yellow luminescence in GaN, Proc. SPIE **6473**, 64730M (2007).
[12] M. Linde, S. J. Uftring, and G. D. Watkins, Optical detection of magnetic resonance in electron-irradiated GaN, Phys. Rev. B **55**, R10177 (1997).
[13] I. A. Buyanova, Mt. Wagner, W. M. Chen, J. L. Lindström, B. Monemar, H. Amano, and I. Akasaki, Optical properties of electron-irradiated GaN, MRS Internet J. Nitride Semicond. Res. **3**, 18 (1998).
[14] C. Bozdog, H. Przybylinska, G. D. Watkins, V. Härle, F. Scholz, M. Mayer, M. Kamp, R. J. Molnar, A. E. Wickenden, D. D. Koleske, and R. L. Henry, Optical detection of electron paramagnetic resonance in electron-irradiated GaN, Phys. Rev. B **59**, 12479 (1999).
[15] G. D. Watkins, K. H. Chow, P. Johannesena, L. S. Vlasenkoa, C. Bozdoga, A. J. Zakrzewskia, M. Mizutab, H. Sunakawab, N. Kurodab, A. Usuib, Intrinsic defects in GaN: what we are learning from magnetic resonance studies, Physica B **340-342**, 25-31 (2003).
[16] K. H. Chow, G. D. Watkins, A. Usui, and M. Mizuta, Detection of Interstitial Ga in GaN, Phys. Rev. Lett. **85**, 2761 (2000).
[17] K. H. Chow, L. S. Vlasenko, P. Johannesen, C. Bozdog, G. D. Watkins, A. Usui, H. Sunakawa, C. Sasaoka, and M. Mizuta, Intrinsic defects in GaN. I. Ga sublattice defects observed by optical detection of electron paramagnetic resonance, Phys. Rev. B **69**, 045207 (2004).
[18] S. Hautakangas, J. Oila, M. Alatalo, K. Saarinen, L. Liszkay, D. Seghier, and H. P. Gislason, Vacancy defects as compensating centers in Mg-doped GaN, Phys. Rev. Lett. **90**, 137402 (2003).
[19] S. Zeng, G. N. Aliev, D. Wolverson, J. J. Davies, S. J. Bingham, D. A. Abdulmalik, P. G. Coleman, T. Wang, and P. J. Parbrook, The role of vacancies in the red luminescence from Mg□ doped GaN, Phys. Stat. Sol. **3**, No. 6, 1919–1922 (2006).

[20] M. A. Reshchikov, D. O. Demchenko, J. D. McNamara, S. Fernandez-Garrido, and R. Calarco, Green luminescence in Mg-doped GaN, Phys, Rev. B **90**, 035207 (2014).
[21] D. W. Jenkins and J. D. Dow, Electronic structures and doping of InN, In x Ga 1− x N, and In x Al 1− x N, Phys. Rev. B **39**, 3317 (1989).
[22] F. Gao, E. J. Bylaska, and W. J. Weber, Intrinsic defect properties in GaN calculated by ab initio and empirical potential methods, Phys. Rev. B **70**, 245208 (2004).
[23] P. Perlin, T. Suski, H. Teisseyre, M. Leszczynski, I. Grzegory, J. Jun, S. Porowski, P. Boguskawski, J. Bernholc, J.C. Chervin, A. Polian, and T. D. Moustakas, Towards the identification of the dominant donor in GaN, Phys. Rev. B **75**, 296 (1995).
[24] J. Neugebauer and C. G. Van de Walle, Atomic geometry and electronic structure of native defects in GaN, Phys. Rev. B **50**, 8067 (1994).
[25] T. Matilla and R. M. Nieminen, Ab initio study of oxygen point defects in GaAs, GaN, and AlN, Phys. Rev. B **54**, 16676, (1996).
[26] C. G. Van de Walle and J. Neugebauer, First-principles calculations for defects and impurities: Applications to III-nitrides, J. Appl. Phys. **95**, 3851 (2004).
[27] M. G. Ganchenkova and R. M. Nieminen, Nitrogen vacancies as major point defects in gallium nitride, Phys. Rev. Lett. **96**, 196402 (2006).
[28] S. Limpijumnong and C. G. Van de Walle, Diffusivity of native defects in GaN, Phys. Rev. B **69**, 035207 (2004).
[29] W. Kohn and L. J. Sham, Self-consistent equations including exchange and correlation effects, Phys. Rev. Lett. **140**, 1133 (1965).
[30] K Laaksonen, M. G. Ganchenkova and R. M. Nieminen, Vacancies in wurtzite GaN and AlN, J. Phys.: Condens. Matter **21**, 015803 (2009).
[31] I. Gorczyca, A. Svane, and N. E. Christensen, Theory of point defects in GaN, AlN, and BN: Relaxation and pressure effects, Phys. Rev. B **60**, 8147 (1999).
[32] O. Gunnarsson, O. Jepsen, and O. K. Andersen, Self-consistent impurity calculations in the atomic-spheres approximation, Phys. Rev. B **27**, 7144 (1983).
[33] J. P. Perdew, Accurate Density Functional for the Energy: Real-Space Cutoff of the Gradient Expansion for the Exchange Hole, Phys. Rev. Lett. **55**, 1665 (1985).
[34] Y. Gohda and A. Oshiyama, Stabilization mechanism of vacancies in group-III nitrides: exchange splitting and electron transfer, J. Phys. Soc. Jpn. **79**, 083705-3 (2010).
[35] Y. S. Puzyrev, T. Roy, M. Beck, B. R. Tuttle, R. D. Schrimpf, D. M. Fleetwood, and S. T. Pantelides, Dehydrogenation of defects and hot-electron degradation in GaN high-electron-mobility transistors, J. Appl. Phys. **109**, 034501 (2011).
[36] Q. Yan, A. Janotti, M. Scheffler, and C. G. Van de Walle, Role of nitrogen vacancies in the luminescence of Mg-doped GaN, Appl. Phys. Lett. **100**, 142110 (2012).
[37] R. Gillen and J. Robertson, A hybrid density functional view of native vacancies in gallium nitride, J. Phys.: Condens. Matter **25**, 405501 (2013).
[38] J. L. Lyons, A. Alkauskas, A. Janotti, and C.G. van de Walle, First□principles theory of acceptors in nitride semiconductors, Phys. Stat. Sol. **252**, 900 (2015).
[39] G. Miceli and A. Pasquerello, Energetics of native point defects in GaN: A density-functional study, Microelectron. Eng. **147**, 51-54 (2015).
[40] A. Kyrtsos, M. Matsubara, and E. Bellotti, Migration mechanisms and diffusion barriers of carbon and native point defects in GaN, Phys. Rev. B. **93**, 245201 (2016).

[41] J. Heyd, G. E. Scuseria, and M. Ernzerhof, Hybrid functionals based on a screened Coulomb potential, J. Chem. Phys. 118, 8207 (2003); J. Heyd, G. E. Scuseria and M. Ernzerhof, Erratum: "Hybrid functionals based on a screened Coulomb potential", J. Chem. Phys. **118**, 8207 (2003).
[42] D. O. Demchenko and M. A. Reshchikov, Blue luminescence and Zn acceptor in GaN, Phys. Rev. B **88**, 115204 (2013).
[43] S. Lany and A. Zunger, Assessment of correction methods for the band-gap problem and for finite-size effects in supercell defect calculations: Case studies for ZnO and GaAs, Phys. Rev. B **78**, 235104 (2008).
[44] C. Freysoldt, B. Grabowski, T. Hickel, J. Neugebauer, G. Kresse, A. Janotti, and Chris G. Van de Walle, First-principles calculations for point defects in solids, Rev. Mod. Phys. **86**, 253 (2014).
[45] D. O. Demchenko, I. C. Diallo, and M. A. Reshchikov, Yellow luminescence of gallium nitride generated by carbon defect complexes, Phys. Rev. Lett. **110**, 087404 (2013).
[46] J. L. Lyons, A. Janotti, and C. G. Van de Walle, Why nitrogen cannot lead to p-type conductivity in ZnO, Appl. Phys. Lett. **95**, 252105 (2009).
[47] J. L. Lyons, A. Janotti, and C. G. Van de Walle, Carbon impurities and the yellow luminescence in GaN, Appl. Phys. Lett. **97**, 152108 (2010).
[48] P. E. Blöchl, Projector augmented-wave method, Phys. Rev. B **50**, 17953 (1994).
[49] G. Kresse and J. Furthmüller, Ab initio pseudopotentials for electronic structure calculations of poly-atomic systems using density-functional theory, Phys. Rev. B **54**, 11169 (1996).
[50] J. P. Perdew, K. Burke, and M. Ernzerhof, Generalized gradient approximation made simple, Phys. Rev. Lett. **77**, 3865 (1996).
[51] R. Dingle, D. D. Sell, S. E. Stokowski, and M. Ilegems, Absorption, reflectance, and luminescence of GaN epitaxial layers, Phys. Rev. B **4**, 1211 (1971); B. Monemar, Fundamental energy gap of GaN from photoluminescence excitation spectra, Phys. Rev. B **10**, 676 (1974).
[52] H. Morkoç, in *Handbook of Nitride Semiconductors and Devices* (Wiley, New York, 2008), Vols. 1–3.
[53] K. T. Jacob and G. Rajitha, Discussion of enthalpy, entropy and free energy of formation of GaN, J. Cryst. Growth **311**, 3806–3810 (2009).
[54] G. Makov and M. C. Payne, Periodic Boundary Conditions in *ab initio* calculations, Phys. Rev. B **51**, 4015-4022 (1995).
[55] F. Oba, A. Togo, I. Tanaka, J. Paier, and G. Kresse, Defect energetics in ZnO: A hybrid Hartree-Fock density functional study, Phys. Rev. B **77**, 245202 (2008).
[56] G. Miceli and A. Pasquarello, Self-compensation due to point defects in Mg-doped GaN, Phys. Rev. B **93**, 165207 (2016).
[57] O. K. Al-Mushadani and R. J. Needs, Free-energy calculations of intrinsic point defects in silicon, Phys. Rev. B **68**, 235205 (2003).
[58] A. M. Stoneham, in *Theory of Defects in Solids: Electronic Structure of Defects in Insulators and Semiconductors* (Oxford University Press, Oxford, 1975), p 296.
[59] D. L. Dexter, C. C. Klick, and G. A. Russell, Criterion for the occurrence of luminescence, Phys. Rev. **100**, 603 (1955).
[60] B. K. Ridley, in *Quantum Processes in Semiconductors*, (Oxford University Press, NY, 2013), p 207.
[61] K. K. Rebane, in *Impurity Spectra of Solids: Elementary Theory of Vibrational Structure*, translated from Russian by J. S. Shier (Plenum Press, New York-London, 1970), pp. 36-54.

[62] A. Alkauskas, Q. Yan, and C.G. van de Walle, First-principles theory of nonradiative carrier capture via multiphonon emission, Phys. Rev. B **90**, 075202 (2014).
[63] L. Shi, K. Xu, and L.-W. Wang, Comparative study of ab initio nonradiative recombination rate calculations under different formalisms, Phys. Rev. B **91**, 205315 (2015).
[64] R. H. Bartram and A. M. Stoneham, On the luminescence and absence of luminescence of F centers, Solid State Commun. **17**, 1593-1598 (1975).
[65] C. H. Leung and K. S. Song, On the luminescence quenching of F centres in alkali halides, Solid State Commun. 33, 907 (1980).
[66] S. Wakita, Y. Suzuki, and M.Hirai, Luminescence Quenching Due to the Dynamical Nonradiative Transition of F Center in KI Crystal, J. Phys. Soc. Jpn. **50**, 2781-2782 (1981).
[67] I. A. Buyanova, Mt. Wagner, W. M. Chen, B. Monemar, J. L. Lindström, H. Amano, and I. Akasaki, Photoluminescence of GaN: Effect of electron irradiation, Appl. Phys. Lett. **73**, 2968 (1998).
[68] W. M. Chen, I. A. Buyanova, Mt. Wagner, B. Monemar, J. L. Lindström, H. Amano and I. Akasaki, Similarity between the 0.88-eV photoluminescence in GaN and the electron-capture emission of the OP donor in GaP, Phys. Rev. B **58**, R 13351 (1998).
[69] A. F. Wright, Interaction of hydrogen with nitrogen interstitials in wurtzite GaN, J. Appl. Phys. 90, 6526 (2001).
[70] H. J. von Bardeleben, J. L. Cantin, H. Vrielinck and F. Callens, L. Binet, E. Rauls and U. Gerstmann, Nitrogen split interstitial center (N− N) N in GaN: High frequency EPR and ENDOR study, Phys. Rev. B **90**, 085203 (2014).
[71] C. Freysoldt, J. Neugebauer, and C. G. Van de Walle, Fully ab initio finite-size corrections for charged-defect supercell calculations, Phys. Rev. Lett. **102**, 016402 (2009).
[72] C. Freysoldt, J. Neugebauer, and C.G. Van de Walle, Electrostatic interactions between charged defects in supercells, Phys. Stat. Sol. B **248**, 1067 (2010).